ForestNavigator

D3.4 Assessment of natural disturbances and extreme events impact on forest mitigation potential

Funded by the European Union

Grant Agreement	101056875
Call identifier	HORIZON-CL5-2021-D1-01
Project full title	ForestNavigator: Navigating European forests and forest bioeconomy sustainably to EU climate neutrality
Work package	WP3
Due date	31/03/2025
Deliverable lead	Andrey Krasovskiy
Authors	Andrey Krasovskiy, Hyun-Woo Jo, Manfred Lexer, Colin Johnstone, Eunbeen Park, Florian Kraxner

Abstract

Deliverable D3.4 presents an integrated modeling approach to assess how natural disturbances—such as wildfires, bark beetle outbreaks, and windstorms—interact with forest management and climate change to affect the carbon sequestration potential of European forests. The model simulates forest growth and disturbance dynamics on an annual time step, incorporating climate sensitivity and management strategies. Projections were carried out under two climate scenarios and three management pathways (i.e., economic, conservation, and societal).

A proof-of-concept application of the new model highlights strong trade-offs between carbon sequestration — assuming harvested woodstores carbon indefinitely — and disturbance exposure, with management scenarios affecting both forest productivity and disturbance risk. Spatial patterns reveal regional hotspots for biomass growth and disturbance damage, providing valuable input for designing adaptive, climate-smart forest policies. This work contributes directly to the ForestNavigator project's objectives by supporting scenario-based decision-making for sustainable forest mitigation and adaptation strategies across Europe.

Keywords

Natural disturbances; Forest management; Carbon sequestration; Climate change; Modeling

Internal Technical Auditor	Name (Beneficiary short name)	Date of approval
Task leader	Andrey Lessa Derci Augustynczik (IIASA)	12/05/2025
WP leader	Manfred Lexer (BOKU)	10/05/2025
Coordinators	Petr Havlík and Fulvio Di Fulvio (IIASA)	10/05/2025
Project Office	Eleonora Tan (IIASA)	12/05/2025

Dissemination level

PU	Public, will be published on CORDIS	✓
SEN	Sensitive, limited under the conditions of the Grant Agreement	

Nature of the deliverable *

	R

Table of Contents

List of Figures

List of Tables

Abbreviations

AWC	Available Water Capacity
CCI	Climate Change Initiative
CWD	Coarse Woody Debris
DBH	Diameter at Breast Height
DEM	Digital Elevation Model
EC	European Commission
ESA	European Space Agency
FAO	Food and Agriculture Organization
FFMC	Fine Fuel Moisture Code
FLAM	Wildfire Climate Impacts and Adaptation Model
G4M	Global Forest Model
GWL	Global Warming Levels
IUCN	International Union for Conservation of Nature
MAI	Mean Annual Increment
NPP	Net Primary Productivity
UNISDR	United Nations International Strategy for Disaster Reduction Secretariat
WP	Work Package

Executive summary

As part of the ForestNavigator project, we developed and applied an integrated forest modeling framework to assess how climate change and forest management strategies interact to shape future European forests. This model simulates forest growth alongside the occurrence of natural disturbances—including wildfires, bark beetle outbreaks, and windstorms—to support informed decision-making on climate adaptation and mitigation, and sustainable forest management.

A key innovation of the model lies in its integration of disturbance and fuel dynamics with forest growth, enabling simulation of realistic post-disturbance pathways and management responses. It operates on an annual time step, is sensitive to weather variability and forest practices, and is spatially explicit, offering potential for both continental and regional-scale insights.

After calibration with historical data, we used the model to project forest growth, natural disturbances, and carbon sequestration under two climate change pathways and three contrasting proof of concept management scenarios:

1. Economic Scenario – Focused on maximizing wood production through timely harvesting and replanting with most productive species.
2. Conservation Scenario – Prioritized biodiversity and ecosystem stability through expanded protected areas and reduced harvest.
3. Societal Scenario – Represented a moderate pathway, balancing conservation goals with socio-economic demands.

Key Findings and Contributions

- Carbon Sequestration and Natural Disturbances:

  The economic scenario resulted in the highest carbon sequestration—assuming harvested wood stores carbon indefinitely. However, it also led to increased damage from bark beetle outbreaks and windthrow in Northern and parts of Central Europe. This is primarily due to the continued dominance of coniferous species under future climate scenarios, especially in the Global Warming Level of 3°C (GWL3) climate scenario.

  In contrast, the conservation scenario resulted in the lowest carbon sequestration due to limited harvesting and lower increments. This scenario shifts towards broadleaf species, which reduces the impacts of bark beetles and windstorms in the North. However, it increases the risk of forest fires in Central and Southern Europe due to fuel accumulation from reduced harvesting.

  The societal scenario resulted in the lowest combined damage from disturbances, likely due to more broadleaf planting than in the economic scenario and more harvesting than in the conservation scenario. This promoted a faster transition to broadleaves and reduced fuel accumulation but led to the lowest standing biomass.

- Disturbance Hotspots and Regional Patterns:

  Biomass increased across Europe, particularly in Western and Southern regions (e.g., France, Italy, Poland) and hotspots of disturbances emerged in Central and Southeastern

Europe (including the Iberian Peninsula and the Balkans). These spatial patterns highlight areas where policy attention and adaptive management may be most urgently needed.

- Management Strategy Implications:

  The results underscore that forest management decisions strongly influence carbon stocks, disturbance vulnerability, and harvest potential. For policymakers, this means that scenario-based planning is essential for balancing trade-offs between carbon sequestration, forest resilience, and resource use.

Relevance to ForestNavigator Objectives

This work directly supports ForestNavigator's mission to provide science-based pathways for climate-smart forest management in Europe. It offers:

- A tool for evaluating adaptation and mitigation strategies at multiple scales by means of quantified projections of biomass, carbon, and disturbance dynamics under future scenarios;
- A foundation for evidence-based policy design that integrates ecological resilience with socio-economic considerations.

By highlighting how different management strategies perform under varying future climate scenarios, our model contributes to navigating forest policy toward EU climate and biodiversity goals, supporting the European Green Deal.

I. Introduction

European forest ecosystems are inherently vulnerable due to the extended lifespan of trees, which hinders their ability to rapidly adapt to abrupt environmental changes. The frequency and intensity of climate-induced disturbances — such as fires, windstorms, and pest outbreaks — are projected to increase significantly with global warming. These events pose a direct threat to critical forest functions, including carbon sequestration and timber production, which may suffer substantially in the near term. Despite the urgency of understanding these vulnerabilities, there remains a significant knowledge gap regarding European forests' susceptibility to multiple climate-related hazards (Forzieri et al, 2020). Natural disturbances, characterized by large-scale tree mortality resulting from abiotic (e.g., fires, strong winds) and biotic agents (e.g., insect outbreaks), represent a serious threat to maintaining healthy and productive forest ecosystems (Forzieri et al, 2020). The intensification of disturbance regimes in Europe is raising concerns about maintaining continuous ecosystem services for human benefit (Patacca, 2022). Considering multiple hazards simultaneously improves decision-making by identifying potential trade-offs and optimizing silvicultural practices. Thus, understanding the vulnerability of the forest systems to multiple disturbances at this interplay is a key determinant of risk, reflecting their susceptibility when exposed to hazardous events.

Wind is recognized as the primary abiotic disturbance agent affecting European forests (Sanginés de Cárcer et al., 2021; Romagnoli et al. 2023). Between 1950 and 2000, windstorms were responsible for approximately 53% of the total damage caused by abiotic agents to European forests, resulting in over 900 million cubic meters (m^3) of windthrown timber—an average annual loss of nearly 18.7 million m^3 (Romagnoli et al. 2023). Projections indicate that windstorms may further increase in frequency of high intensity windstorm, exacerbating forest vulnerability and exposure (Romagnoli et al. 2023).

The interplay between an elevated volume of salvageable timber from windstorm events and extended periods of drought enhances the susceptibility of these ecosystems to bark beetle infestations (Seidl and Rammer, 2017; Berčák et al, 2023). This phenomenon is particularly evident in coniferous forests across the Northern Hemisphere, where bark beetle populations have surged over the last four decades. Europe has been notably affected by recent bark beetle outbreaks, which are often regarded as significant societal challenges. These infestations not only alter forest ecosystems but also leave lasting imprints on their structure and appearance. For instance, if the quantity of wind-damaged timber is too extensive to manage promptly, it fosters an environment conducive to bark beetle proliferation. Damaged trees are ideal habitats for these beetles, especially under favorable weather conditions that support their reproduction and survival (Berčák et al, 2023). Furthermore, windstorms and bark beetle infestations can mutually reinforce each other and follow one another, leading to cascading disturbances within forest ecosystems (Berčák et al, 2023).

Wildfire risk is a growing concern across EU territories, demanding proactive management strategies (Cunningham et al., 2024; Fernandez-Anez et al., 2021; Robinne et al., 2018; IUCN and UNEP-WCMC, 2022; Rossi et al., 2020). Climate change exacerbates wildfire risks, underscoring the need to prioritize this issue in both EU and international agendas (EC, 2023; European Environment Agency, 2024; UNISDR, 2015). Several key policies and strategies address wildfire management, including the Nature Restoration Law (EC, 2024), the EU Biodiversity Strategy 2030 (EC, 2020), and the EU Green Infrastructure Strategy (EC, 2013). These initiatives emphasize nature-based solutions, focusing on fuel management, conservation, forest protection, and the restoration of fire-adapted ecosystems to their natural fire regimes. Furthermore, fire causes significant alterations in vegetation cover and environmental conditions, such as changes in soil moisture content, microclimate near the ground surface, and irradiance levels (Kučerová, 2008).

Accurately assessing wildfire risks and their impact on forest growth and biodiversity requires precise modeling of available fuel, primarily deadwood, which influences fire occurrence, spread, and intensity (Larjavaara et al.., 2023) while also serving as an important biodiversity indicator. Modeling the dynamics of fuel moisture content further enhances fire risk assessment, especially in protected forests (Arellano-del-Verbo et al., 2023) and supports the development of adaptive strategies such as fuel management and fire-smart forestry practices (Fernandes, 2013; Hirsch et al., 2001; Tedim et al., 2016).

This modeling task analyzes forest growth across Europe under climate change and varying management strategies, generating three stylized scenarios of future development aligned with potential policies. The focus is on the future development of natural disturbances (wildfire, bark beetle, and windstorms) and their impacts on forest carbon stock. Achieving this requires high-resolution modeling of forest growth and predicted damage from natural disturbances.

In this task, we developed a dynamic disturbance module combining three mechanistic algorithms: wildfire climate impacts and adaptation model (FLAM), and bark beetle and windstorm algorithms from PICUS. We also developed a fuel module that integrates a global forest model (G4M) with a disturbance module at an annual time step, simulating both disturbances and post-disturbance management. We constructed three management scenarios that reflect potential directions in forest management, linked to climate change projections through 2070. Finally, we evaluated the impacts of these scenarios using carbon in harvested andstanding stemwood biomass, as well as losses from disturbances. This methodological approach enhances our ability to assess the effects of policies on forests across Europe.

2. Methods

The ForestNavigator forest and natural disturbances modeling suite comprises three models: a global forest model (G4M) to simulate the dynamics of forest growth, the wildfire climate impacts and adaptation model (FLAM), and bark beetle and windstorms algorithms from the PICUS model. The disturbance module has been developed to assess the risks of three natural disturbances: fire, bark beetle, and windstorm. Additionally, a fuel module has been developed that facilitates dynamic interaction between natural disturbances module and the global forest model (G4M).

2.1. Wildfire Climate Impacts and Adaptation Model (FLAM)

The wildfire climate impacts and adaptation Model (FLAM) captures the effects of climate, human factors, and fuel availability on ignition probability, fire spread, and burned areas. FLAM uses a process-based fire parameterization algorithm initially developed to link fire modeling with dynamic global vegetation models (Arora and Boer, 2005). By coupling this algorithm with Fine Fuel Moisture Code (FFMC) calculations (Wagner and Pickett, 1985), FLAM predicts burned areas by considering both ignition probability and suppression efficiency. FLAM represents wildfires more accurately under varying conditions due to its ability to calibrate suppression efficiency, unlike models with fixed suppression parameters (Krasovskii et al., 2016). The model has been successfully applied in Europe, Indonesia, South Korea, and boreal forests (Khabarov et al., 2016; Krasovskii et al., 2018; Jo et al., 2023; Corning et al., 2024) among other regions. The primary focus of FLAM modeling is the identification of wildfire hotspots under historical, current, and future conditions, as well as the projection of burned areas under various climate change scenarios and management strategies. FLAM can also model adaptation options, such as prescribed burning, fuel removal, and enhanced suppression efficiency, including improved reaction times. The FLAM general scheme is shown in Figure 1.

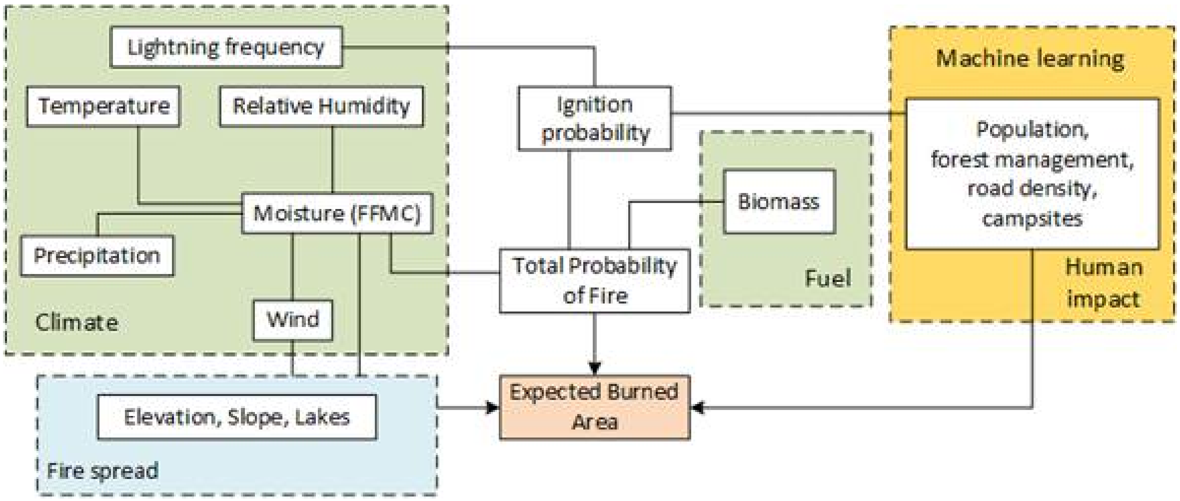

Figure 1: FLAM workflow (Source: https://iiasa.ac.at/models-tools-data/flam)

FLAM is calibrated and validated using the most recent publicly available GIS and remote sensing datasets. FLAM's modular structure allows for the integration of additional fire ignition and propagation drivers, such as topography, socio-economic factors, and proximity to agricultural land. In this study, FLAM has been integrated with IIASA's G4M to comprehensively assess biomass growth and wildfire damage interactions, achieved through a dynamic fuel module that facilitates model interaction.

2.2. Global Forest Model (G4M)

The G4M simulates the changes in the properties of forests on large scales, including the effects of forest growth, mortality, regeneration, and management, with the latter including thinning, harvests, and replanting (Kindermann et al., 2013). Typically, the model considers geographical areas covering entire countries or continents and breaks down the geographical area being considered into a finite set of pixels. Within each pixel, the forests are broken down into components based on species and for each species, they are broken down further into even-aged cohorts. The species categories included in this study are coniferous pioneers, slow-growing coniferous, Mediterranean coniferous, fast-growing deciduous, slow-growing light-demanding deciduous broadleaf, slow-growing shade-tolerant deciduous broadleaf, and evergreen broadleaf.

The model for growth productivity is an important component, which in G4M is represented as theoretical net primary productivity (NPP) in units of tC ha^{-1} $year^{-1}$. For each species, a monthly average value is calculated within each pixel, which can vary annually based on changes in the climate and soil input parameters. The climate parameters used are air temperature, precipitation, and incident solar radiative flux. The soil parameters are water holding capacity, nitrogen and phosphorus contents, acidity, and salinity. Additionally, atmospheric CO_2 concentration and pressure (depending on altitude) are included. These are used in a regression model fitted to aggregated MODIS NPP data (MOD17A2HGF v006) and for each species and ecoregion (i.e. tropical, subtropical, temperate, and boreal). The monthly averaged NPP values are then converted into yearly averaged mean annual increment (MAI) values for use in G4M's growth model.

The growth model consists of a set of empirical regression equations that describe the yearly changes in living stemwood biomass per hectare, tree diameter, and tree height as functions of species, age, productivity (MAI), and stocking degree. With this growth model, we can also calculate quantities relevant for management decisions, such as the rotation time that maximizes the mean increment. Within each forest type, it is possible to distinguish between slow, average, or fast culminating species. At the local or regional scale, the growth pattern of some tree species like spruce, beech, fir, oak, or pine is explicitly represented in the model, but yield estimates need to be provided by external sources.

The forest structure within each pixel is represented as a series of even-aged and single-species cohorts, and the productivity and growth models are combined to calculate the changes in the properties (biomass, average diameter at breast height (DBH), and average height) in these cohorts. The living stemwood biomass per hectare is additionally influenced by thinning in managed forests. Each cohort is associated with a specific area, which is influenced by natural mortality and harvesting, both of which typically return the cohort's area to an age of zero years, representing reforestation (Figure 2). Depending on the management and climate parameters this reforestation can be with the same or a different species. Simulated forest managers decide on thinning intensities, when to harvest, how much to harvest from each species, cohort, and region, and which species to select for regeneration.

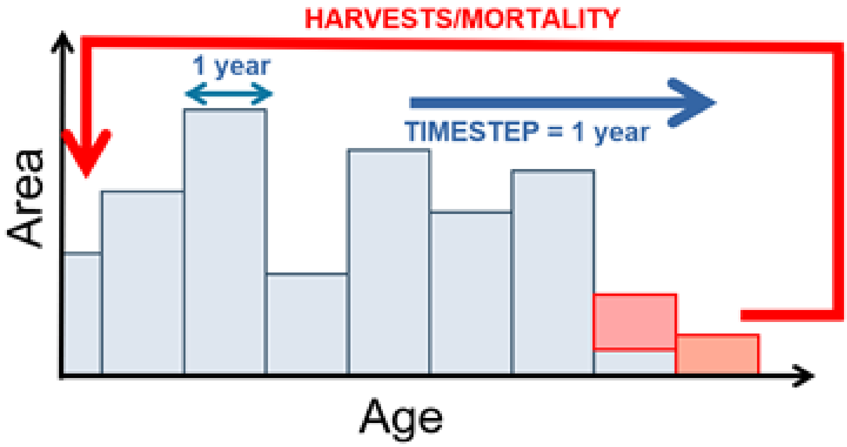

Figure 2: Diagram demonstrating the core algorithm of G4M. For each species the forest structure in a pixel is represented as a set of even-aged cohorts, each covering an area of the pixel. This distribution shifts to older ages each year (blue arrow), and both harvests and natural mortality remove area from the oldest cohorts (red areas). New zero-aged cohorts are added at the start of each with an area equal to everything removed from the older cohorts in the previous year.

For each year and species, the final output of G4M includes the simulated age structure of the forest, the total amount of harvested wood, harvest residuals, and the amount of wood killed by natural mortality and disturbances. Each of the modules and the order of computation within G4M are demonstrated in Figure 3.

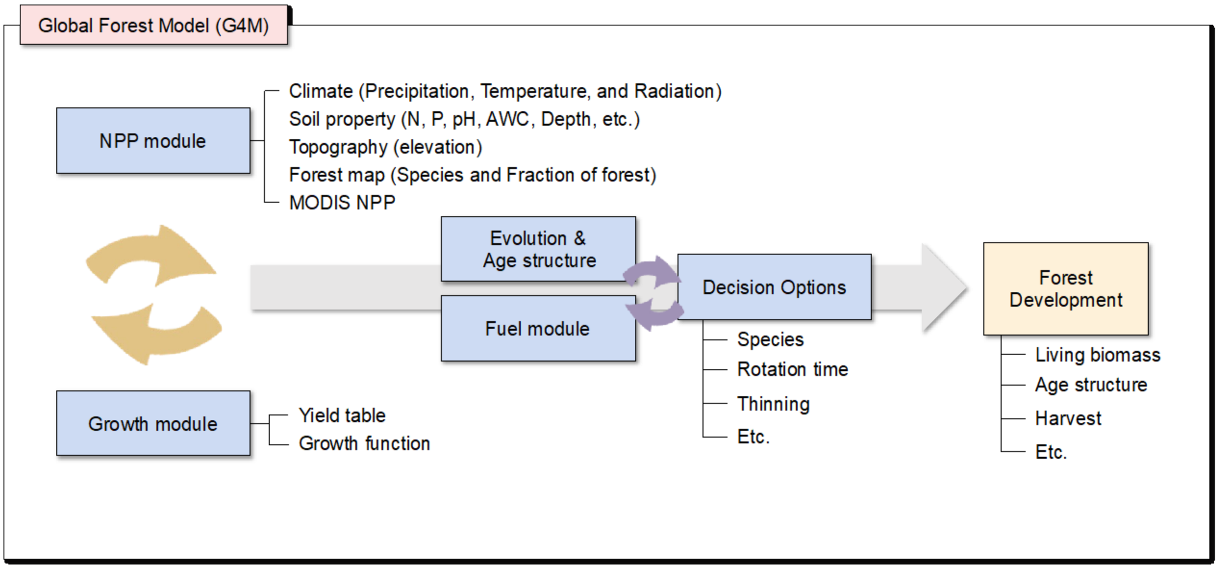

Figure 3: Demonstration of all modules in the full G4M model leading to time-dependent forest properties.

2.3. PICUS algorithms for bark beetle and windstorms

In the PICUS model, a spruce bark beetle disturbance module had been part of the tree mortality processes from the very first model versions on (Lexer and Hönninger 1998). The early bark beetle disturbance versions were later refined and enhanced by Seidl et al (2007). A further major step in model development history was the integration of a storm damage module, which interacted with the bark beetle disturbance module. A more recent version was based on work by Pastor et al. (2014, 2015).

Bark beetle disturbance module

The bark beetle disturbance module is a process-based module which builds on two elements. First, the probability of a damage event is calculated via the predictors volume share of Picea abies, crown closure based on the basal area, mean stand age, drought conditions via a soil moisture index, the number of bark beetle generations per season and the damage from the previous four years from wind and bark beetle disturbances. A random number decides whether a damage event is triggered or not. In the case of a damage event, the damage intensity (number of stems/ha killed by bark beetles) is estimated by the share of Picea abies in the stand, the drought conditions, and the cumulated bark beetle damage from the previous four years. Figure 4 displays the core module logic.

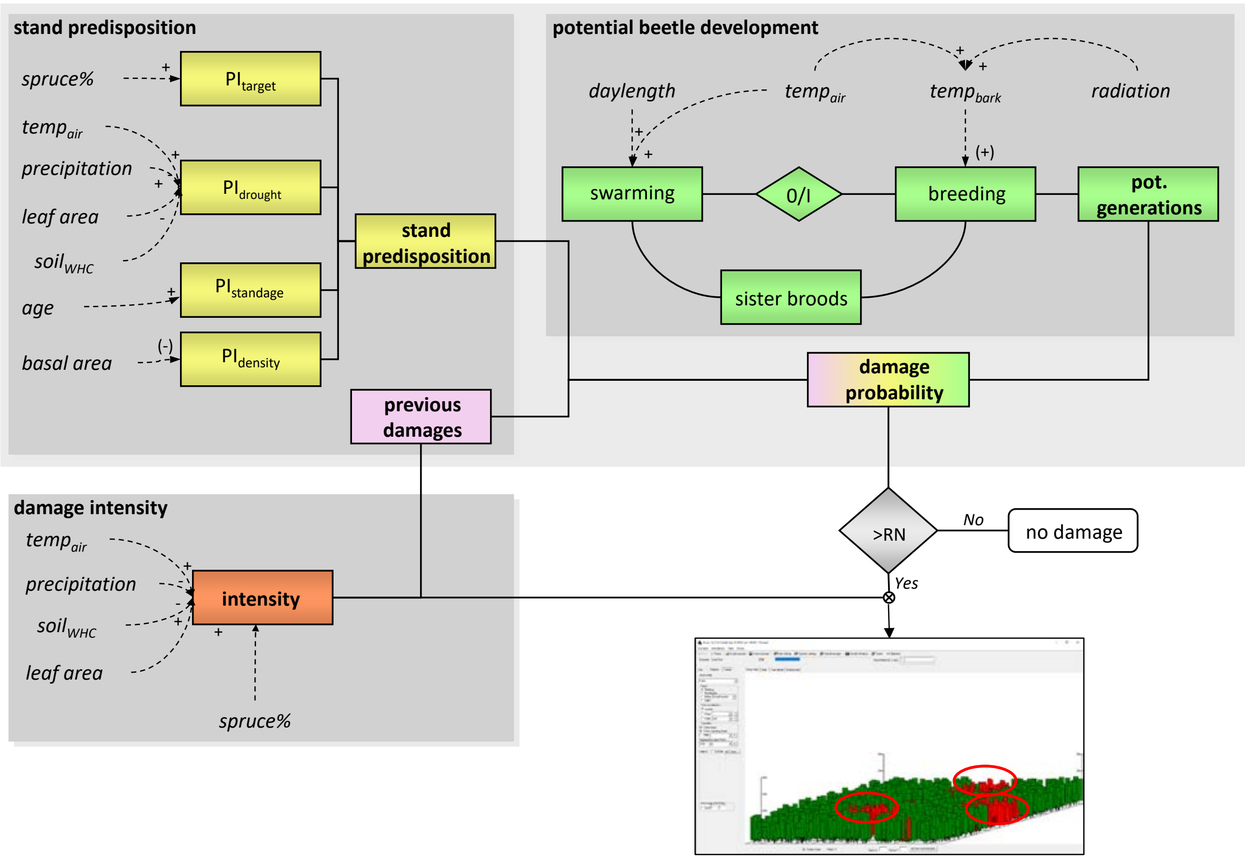

Figure 4: Major elements and interactions of the bark beetle disturbance module in PICUS.

Wind disturbance module

The wind disturbance module utilizes daily maximum wind gust speed, climate, and stand-specific data to predict the occurrence and impact of stand-damaging wind events. The process is structured as follows. First, the probability of a damage event is calculated. The probability of a damage event is estimated from the predictor variables: highest daily wind gust speed per season, mean stand age, volume, frozen soil state, and the damage from the previous four years from wind, bark beetle, and snow damages. A random number decides whether a damage event occurs or not. Second, the damage intensity is calculated based on a mean estimate from a linear regression model, which includes the predictor variables volume share of Picea abies, timber stock and the damage from the previous four years from wind disturbances. A stochastic element drawn from a beta distribution is added to the mean estimate to account for the huge variability in storm damages, which cannot be accounted for by regression analysis. The algorithms and equations are based on Pasztor et al. (2015). Figure 5 displays the major elements and interactions of the storm disturbance model.

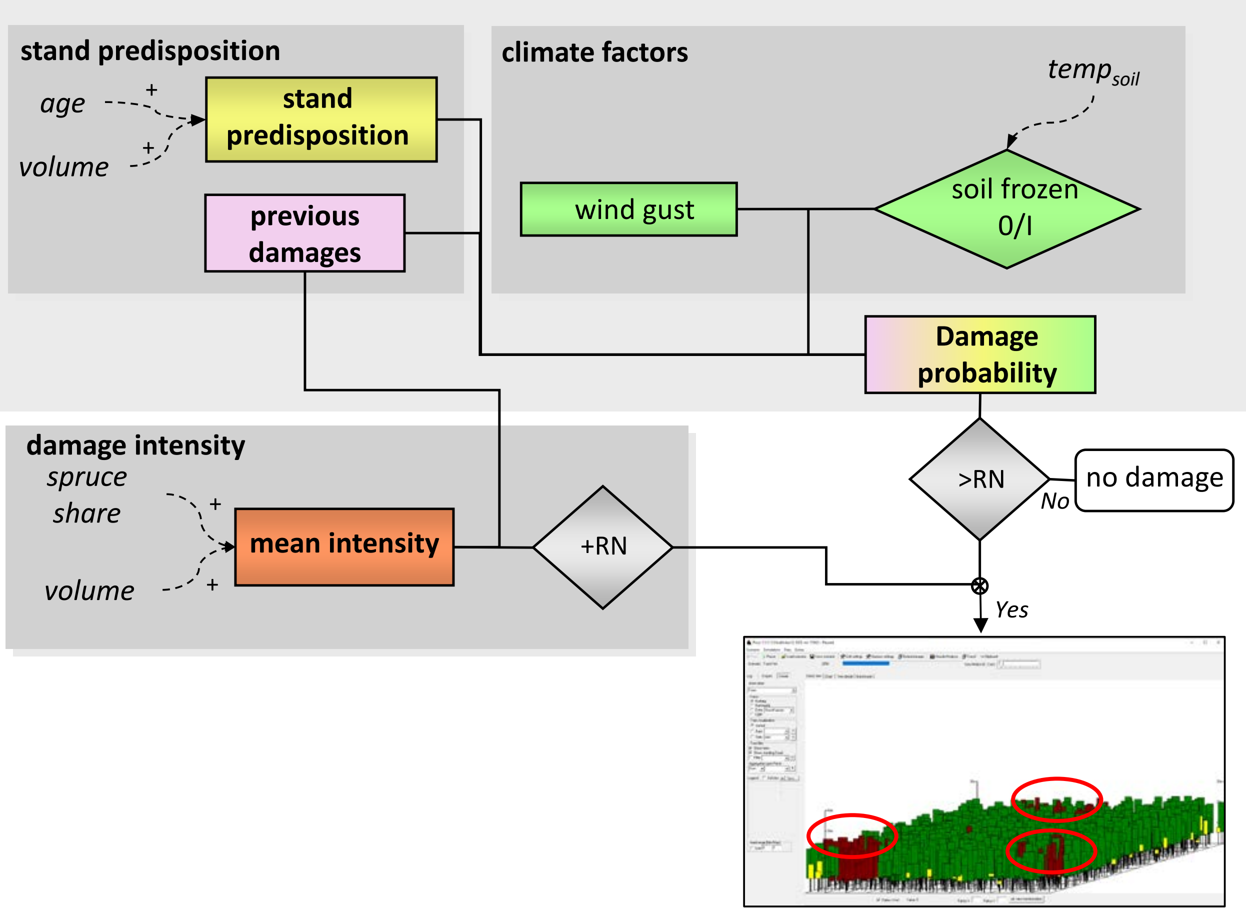

Figure 5: Major elements and interactions of the storm disturbance module in PICUS.

2.4. Integrated modeling approach

The forest dynamics and disturbance module are interconnected through a dynamic integration process facilitated by a newly developed fuel module. Outputs from this combined model — including forest structure variables from G4M, as well as burned areas and fire intensity from FLAM and damages from bark beetles and windstorms — are exchanged between the modules at an annual step. The workflow is shown in Figure 6. G4M simulates forest growth and provides necessary information to the fuel module, which in turn generates annual input for the disturbance module in terms of deadwood (i.e., coarse woody debris (CWD)) and litter components. G4M also gives the necessary forest structure variables to PICUS components. The disturbance module provides forest damage for G4M to update the forest state in the next step. Simultaneously, it gives information on fuel removal to the Fuel module.

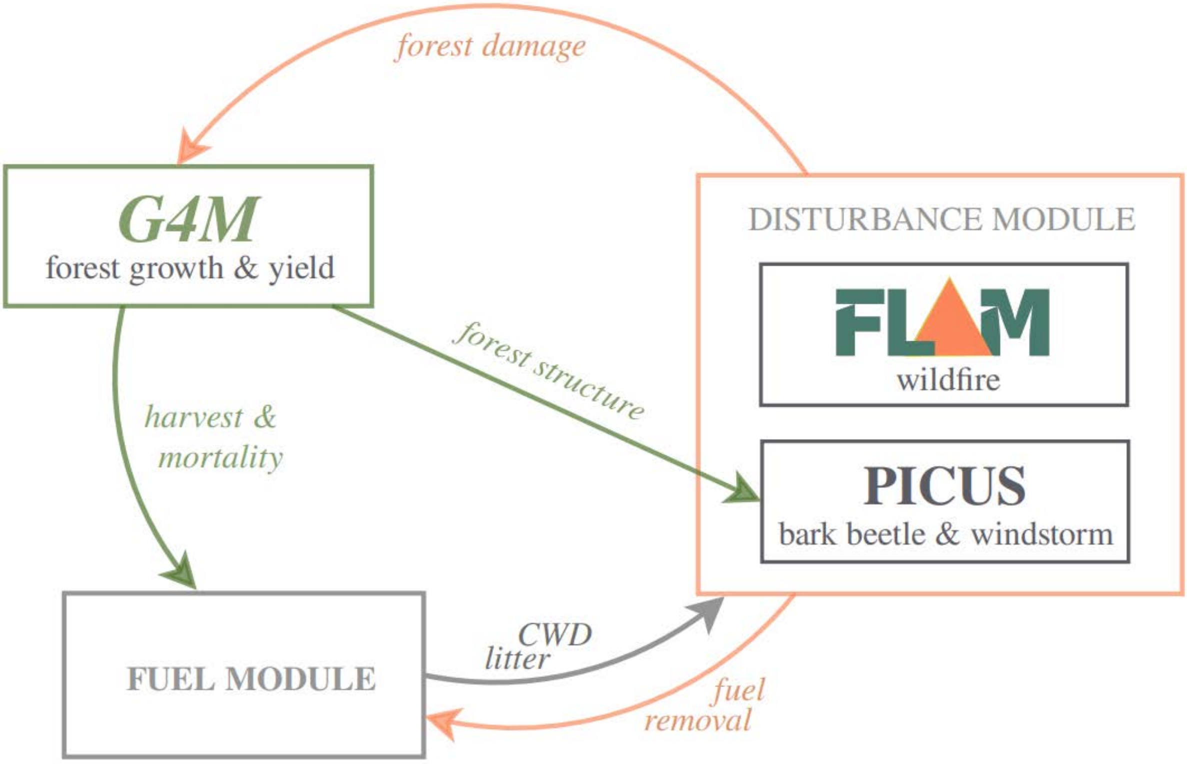

Figure 6. Modeling workflow.

Note that this version of G4M is exclusively a biophysical model, which excludes any economic optimization of forest management and therefore cannot simulate exogenous targets, such as the LULUCF emission targets, allocate exogenous demand for timber products based on market dynamics, or responses of forest managers to changes in growth or disturbance. We have developed a dynamic interaction between the biophysical G4M and disturbance module described in Section 2.6. This is a first step towards integrated assessment of the impact of alternative land-use policies on forest management that account for the interactions between forest management, climate change and disturbances on forest dynamics, productivity and market feedbacks, which will be enabled in the future by coupling with G4M-X and GLOBIOM within this project.

2.5. Study area and biophysical modeling input data

In this study, we focused on all EU forests land in the EU-27 countries. EU forests are represented in a uniform grid with a resolution of 5 arc minutes, corresponding to approximately 8 square kilometers per pixel. All input data was pre-processed to match this resolution.

The input data required by FLAM is listed in Table 1. FLAM requires daily weather to assess fuel moisture content, the fuel in this study is provided via the developed fuel module.

Table 1: Input data required by FLAM

Variable	Unit	Frequency	Source
Temperature	Degrees Kelvin or °C	Daily	Meteo climate data
Wind speed	km/h	Daily	Meteo climate data
Precipitation	Meters	Daily	Meteo climate data

Relative humidity	%	Daily	Meteo climate data
Fuel	gC/m^2	Yearly	Fuel module (G4M+FLAM)
Landcover	Type	Once or yearly	ESA WordCover
Population density	$People/km^2$	Once or yearly	(Warszawskie et al., 2016)
Observed burned area	ha	Monthly	MODIS FireCCI51

Source: ForestNavigator WP 3

The input data used by the G4M model is given in Table 2. It requires weather, topology, as well as soil information and parametrization for the main forest types.

Table 2: Input data required by G4M

Variable	Unit	Required Unit	Frequency	Source
Precipitation	mm/month	mm/month	Monthly	Meteo climate data
Temperature	°C	°C	Monthly	Meteo climate data
Solar radiation	W/m^2	W/m^2	Monthly	Meteo climate data
Digital elevation model (DEM)	m	m	Once	U.S. Geological Survey (USGS,1996)
Soil phosphorus	gP/m^2	gP/m^2	Once	(Yang et al.,2013)
Soil salinity	dS/m	dS/m	Once	HWSD v1.2 (Fischer et al., 2008)
Soil bulk Density	Cg/cm^3	-	Once	SoilGrid
Soil depth	cm	-	Once	SoilGrid
Soil nitrogen	Cg/kg	t/ha (considering soil depth)	Once	SoilGrid
Soil pH	10pH	pH	Once	SoilGrid
Soil available water capacity (AWC)	Type	mm (considering soil depth)	Once	HWSD v1.2 (Fischer et al., 2008)
Land cover map	Type	Type	Once or yearly	CGLS-LC 100 (Buchhorn et al., 2020)
Growth curve parameters	-	-	Once	Kindermann et al. (2013)
NPP parameters	-	-	Once	Kindermann et al. (2013
Age structure*	-	- (considering species and forested fraction cover)	Once	Pucher et al. (2022)
Forest Species fractional cover*	-	-	Once	Pucher et al. (2022)

Variable	Unit	Required Unit	Frequency	Source
Forest protection area*	-	-	Once	Protected Planet (IUCN and UNEP-WCMC, 2022)
Harvested amount*	m^3	-	Once or yearly	FAO (2024)
				*Optional data

Source: ForestNavigator WP 3

Table 3 lists the input data required by the PICUS model, which includes weather conditions and forest structure information, particularly requiring spruce species.

Table 3: Input data required by PICUS

Variable	Unit	Frequency	Source
Avg. Temperature	Degrees Kelvin/°C	Daily	Meteo climate data
Max. Temperature	Degrees Kelvin/°C	Daily	Meteo climate data
Radiation	Wh	Daily	Meteo climate data
Wind gust	km/h	Daily	Meteo climate data
Soil moisture	%	Yearly	FLAM (Meteo climate data)
Age structure	(considering species and forested fraction cover)	Yearly	G4M
Basal area	m^2/ha	Yearly	G4M
Litter mass	Cg/m^2	Yearly	G4M
Biomass density	m^3/ha	Yearly	G4M
Leaf Area Index (LAI)	-	Yearly	G4M

Source: ForestNavigator WP 3

For meteorological and climate data, we used three EUROCORDEX climate models (Jacob et al., 2014) representative for two Global Warming Levels (GWL): GWL2.0: MPI-M-MPI-ESM-LR_rcp45_r1i1p1_CLMcom-CCLM4-8-17, and GWL3.0: MPI-M-MPI-ESM-LR_rcp85_r1i1p1_CLMcom-CCLM4-8-17. They correspond to RCP scenarios 4.5 and 8.5 (van Vuuren et al., 2011), respectively. Daily values for the variables listed in Tables 1 – 3 were used for both historical and future periods.

2.6. Development and integration of disturbance modules and G4M

In this section, we outline the key methodological advancements of the G4M and FLAM models completed as part of the ForestNavigator project and describe the main calibration and optimization procedures used to align them with historical data for Europe. Notably, PICUS algorithms were integrated into the FLAM model, enhancing its capacity to simulate combined bark beetle and windstorm disturbances (together with wildfires). A significant step was also made with the development of a new fuel model, designed to support the dynamic interaction between the G4M and FLAM models. Furthermore, G4M was enhanced to incorporate exogenous, spatially explicit forest management, allowing for the specification of regional or national harvest targets.

These improvements collectively enable an analysis of forest dynamics, including damages from disturbances under varying climate and management conditions.

FLAM receives fuel input generated by G4M and returns burned area estimates. The FLAM and G4M models are linked on an annual basis, because FLAM operates on a daily time step, while forest structure in G4M evolves on an annual time step. The interaction between the models is implemented in a spatially explicit manner, meaning it is applied to each pixel in the grid.

The workflow shown in Figure 7 consists of the following steps:

1) G4M initializes input into the fuel module.
2) FLAM runs at a daily step using fuel available for burning and generates burned area that accumulates over the year.
3) PICUS runs based on forest structure information from G4M and generates annual damage from bark beetles and windstorms.
4) G4M updates forest structure using combined damage from natural disturbances and runs for the following year.

Since fire ignition often originates in grasslands and croplands, we incorporated these fuel types using data from IIASA's EPIC model (Lauerwald et al., 2023). Additionally, we included shrubland, which is not explicitly modeled in EPIC but is parameterized in G4M to represent a significant vegetation type for fire ignition and spread in Europe. The area of each vegetation type was derived from the Copernicus global land cover product (Buchhorn et al., 2020), while fuel density per area was modeled using data from both EPIC and G4M.

The newly developed fuel module (see Figure 7) evolves the carbon surface densities of deadwood and litter considering the effects of background accumulation, mortality, decomposition, harvests, and disturbances. The fuel is assumed to consist of a fast decomposition component, corresponding to the litter, and a slow decomposition component, corresponding to CWD. In the new fuel module, background accumulation for the slow and fast decomposition components happens from each of the living components of the forest, with the contributions of each species category depending on their total biomass within the pixel. Additionally, the module also considers management options within the G4M framework that involves harvesting and different planting options for different management scenarios, which in turn influences the growth of the living component and therefore fuel and fire ignition dynamics. Each component is described as a pixel average carbon surface density in tC ha^{-1}.

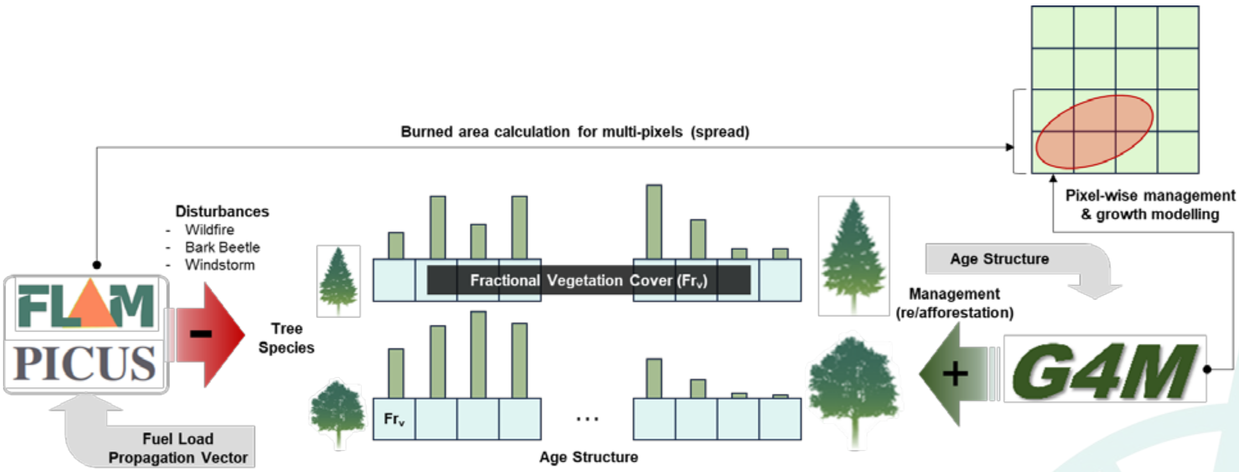

Figure 7: Integration scheme of disturbance module and G4M

We assume that decomposition removes carbon at a rate proportional to the surface density of carbon in the fuel, with assigned rates for the slow and fast decomposition components, respectively. Background accumulation is assumed to add fuel at a rate that is proportional to the total living biomass in the pixel. Harvests influence the model by leaving a certain amount of fuel on the ground. The effects of harvests and disturbances come naturally from the G4M model. An important parameter in determining the effects of disturbances is the fraction of killed carbon that remains in the forest as deadwood. The difference in the fuel evolution post-disturbance for the extreme cases of all killed carbon being removed and all killed carbon remaining in the forest is shown in Figure 8. These cases are used to demonstrate the range of possible behaviors of the fuel dynamics in the model, and our model is flexible for how much of the carbon is killed in a disturbance and how much of that is left in the forest post-disturbance.

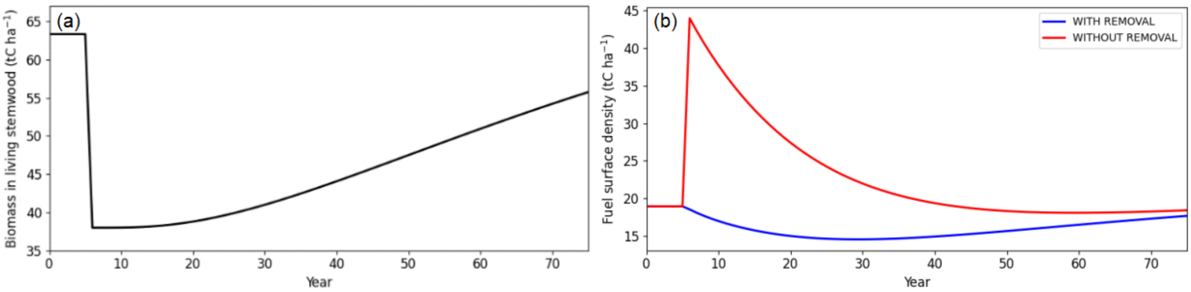

Figure 8: (a) Example simulation showing the evolution of living stemwood biomass after a fire that kills 40% of the living biomass and (b) the corresponding evolution of the total fuel (CWD and litter) surface densities. As a demonstration of the model, we assume the extreme cases of no removal of killed carbon (red) and removal of all killed carbon (blue).

2.7. Methodology for calibration of the models

Country-level calibration of forest productivity and age structure

In G4M, forest productivity and age structure at the pixel level govern biomass increment over time. To align the model with observed data, pixel-wise forest productivity and age structure were calibrated for each species across age classes ranging from 1 to 200 years. The calibration aimed to reproduce country-level living stem biomass statistics (FAO, 2020).

Forest productivity, initially estimated from environmental variables (Section 2.5), was adjusted to match observed biomass increments during the calibration period. Age structure was fine-tuned by skewing the distribution toward younger or older cohorts, using Pucher's et al. (2022) approximate age structure as a baseline, in order to minimize bias.

Data-driven harvest intensity and protected forest modeling

The historical harvest amounts for each country were derived from the Forestry production and Trade of FAO statistics (FAO, 2024). The baseline for future projections is based on an average of the most recent five years, adjusted according to each management scenario. The annual harvest amount was then spatially allocated to grid cells proportionally to the square of the living stem biomass at the national level, excluding protected areas, to prioritize harvesting in mature forests.

For existing protected areas we used data from the Protected Planet database, considering only protected areas in International Union for Conservation of Nature (IUCN) categories I to III, where timber harvest for commercial purposes is generally not allowed, (IUCN and UNEP-WCMC, 2022).

Forest area under this protection regime constitutes 8.17% of the total forest area in the study region.

Calibration of suppression efficiency using machine learning

FLAM's ability to calibrate suppression efficiency enables it to represent wildfires more accurately under varying conditions. In this study, we advanced the suppression efficiency algorithm by incorporating both spatial adjacency and biophysical features, which can dynamically adjust based on future fuel and population conditions.

The new algorithm optimizes spatially explicit suppression efficiency based on the adjacency of the cells as well as their features, including population density, fuel, and topography. The calibration is performed on historical burned areas from the European Space Agency's (ESA) MODIS FireCCI51 product (Chuvieco et al., 2018, 2019). The algorithm uses ensemble multiple segmentation. The new approach significantly improves model performance on a monthly step. The illustration of the algorithm is depicted in Figure 9. It shows the optimization process that compares observed burned areas with primary model prediction in both spatial and intertemporal dimensions. Here, primary predictions are obtained by default model runs with fixed suppression efficiency. The FLAM model, enhanced with the new fuel module, operates on a daily timestep, and the simulated burned areas are aggregated into monthly outputs to align with the observed burned area data. A machine learning algorithm is used to model suppression efficiency, taking into account features of adjacent cells, including population density, fuel type, and topography. This approach allows for the optimization of suppression efficiency and enables spatial assessment based on the characteristics of a given location. This algorithm uses a stochastic approach to wildfire events, which helps capture large-scale occurrences.

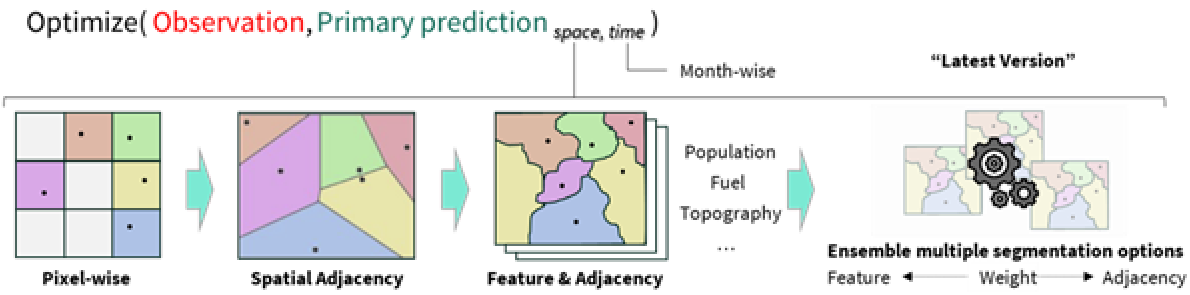

Figure 9: Diagram illustrating the process of optimizing suppression efficiency.

Calibration of bark beetle and windstorms

The calibration of the disturbance module focused on tuning two key components: (1) a transformation coefficient that converts bark beetle-affected trees into merchantable damaged volume, and (2) a probabilistic function representing windstorm-induced damage, accounting for stochastic variability and stand vulnerability. These parameters were systematically adjusted to align the model's annual disturbance output with historical reference data. Rather than fitting to specific events, calibration emphasized matching the magnitude and variability of observed damages over time, using a reference range of 30–70 million m^3 per year derived from multiple pan-European sources (Fernandez-Carrillo et al., 2020; Reimann, 2019; Radio Prague International, 2020).

This calibration process was performed in dynamic linkage with G4M, ensuring that variations in forest structure—such as species composition, age class, and standing volume—were accurately propagated into the disturbance module. Particular care was taken to maintain consistency in forest growth and harvest assumptions, so that the disturbance outputs would remain sensitive to realistic forest development trajectories rather than artificial input fluctuations. The calibration phase was iterative, involving repeated simulation cycles and visual validation with statistical reports and spatial outbreak records, ensuring that the resulting damage trends were quantitatively credible and spatially coherent.

2.8. Stylized forest management scenarios under future climate change

To explore the implications of different management regimes, we considered the following three stylized scenarios for forest management in Europe under climate change:

1. **Conservation Scenario**: This scenario focuses on enhancing biodiversity in Europe's forests. It assumes an extended rotation period for all tree species, leading to a 20% reduction in current harvest intensity relative to historical harvest levels used to calibrate the model. For reforestation following harvests or stand-replacing fires, broadleaf species are prioritized, comprising up to 60% of new plantings. After harvest or disturbances, forests are reforested with broadleaf species to reach the targeted proportion. No specific broadleaf species is prioritized; instead, all broadleaf species are planted evenly until the target is met. Additionally, protected areas where no commercial timber harvesting is allowed are expanded from ~8% in the present to cover 20% of the total forest area. The increase in protected areas is concentrated around historically protected zones.
2. **Economic Scenario**: This scenario aims to maximize carbon sequestration and harvest yields. It assumes maintaining current harvest intensity, prioritizing the most productive tree species for planting, and leaving protected area coverage unchanged.
3. **Societal Scenario**: This scenario prioritizes local consumption and climate-smart management. It assumes a 10% reduction in harvest intensity, an increase in the proportion of broadleaf species to 50%, and an expansion of protected areas to cover 10% of the total forest area. The Societal Scenario is effectively an intermediate scenario between the first two.

To illustrate these scenarios, we provide infographics in Figure 10.

Additionally, the three scenarios were tested under two future climate scenarios until year 2070:

- GWL2, a scenario consistent with RCP 4.5 (medium climate change impact)
- GWL3, a scenario consistent with RCP 8.5 (high climate change impact)

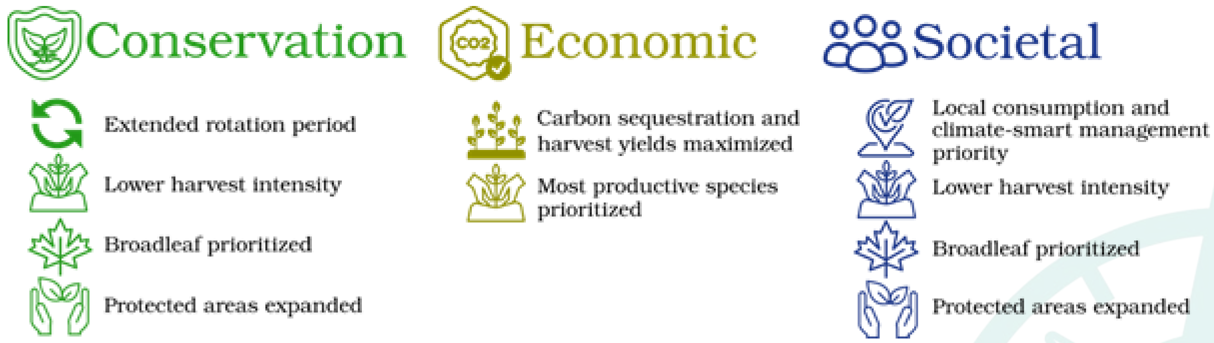

Figure 10: Scenario Infographics. (Graphics source data: https://www.iconrepo.com/)

3. Results

This section presents modeling results for both the historical period (2001–2020) and future projections (2021–2070) under the two climate change and three forest management scenarios outlined in Section 2.8.

3.1. Calibration and validation of the integrated model

Both the FLAM and G4M models are calibrated using historical input data and observations. The integrated model was optimized to align with historical trends in burned area and forest biomass statistics.

Dynamics of forest disturbances

Burned area observations were derived from the FireCCI51 burned area product v5.0, developed under the ESA Climate Change Initiative (CCI) Program, covering the period from 2001 to 2020. The data, originally at a 250-meter resolution, was aggregated to a 5-arc-minute grid for forest, shrubland, and grassland areas. This observed burned area data was used to calibrate and validate FLAM, enhanced by the new fuel module, during the historical period. The calibrated suppression efficiency was then applied to future projections, alongside daily weather scenarios and forest growth data modeled by G4M.

A key feature of FLAM is its capacity to calibrate spatial fire suppression efficiency to better capture month-to-month burned area dynamics in historical data. As outlined in section 2.7, this calibration process involves comparing observed and modeled burned areas over time to adjust FLAM parameters in alignment with the average burned area per pixel. Following calibration, the model is re-evaluated focusing on monthly burned area accuracy. Finally, validation tests assess FLAM's performance in modeling monthly burned areas, as illustrated in Figure 11. The calibration period was set at the start and end of the historical period from 2001 to 2005 and from 2016 to 2020. FLAM successfully reproduced the monthly trends in burned area observed in the FireCCI dataset. While the overall annual trend in observed burned area is declining—primarily due to improved land management in grassland and agricultural areas over recent decades (as reported in GFED5 (Chen et a., 2023))—FLAM does not attempt to model changes in suppression efficiency for these land cover types. This is due to the high uncertainty in projecting future improvements in management practices. Consequently, FLAM's projections show an increasing trend in burned area, driven primarily by the impacts of climate change.

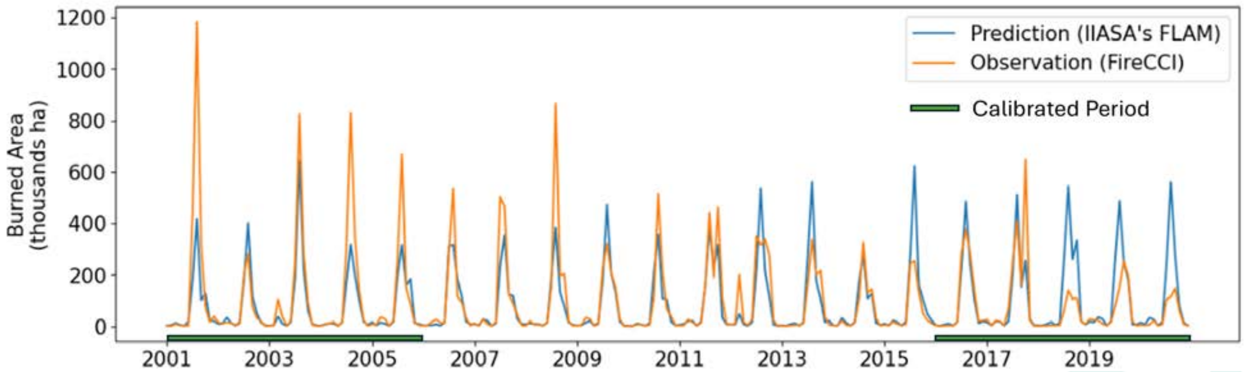

Figure 11: Monthly dynamics of burned area across EU-27 modelled by FLAM and reported by FireCCI product

Bark beetle and windstorm damages were not simulated in a stand-alone setting, as their inputs depend on outputs from other models, making independent execution infeasible. As a result, a significant portion of the projected damages—particularly their interannual trends—is influenced by the calibration of G4M, which supplies key forest structural information to PICUS algorithms.

Despite this dependency, the calibration of annual damage levels successfully reproduced pan-European disturbance estimates ranging from 30 to 70 million m^3 (Fernandez-Carrillo et al., 2020; Reimann, 2019; Radio Prague International, 2020). Moreover, the peak disturbance observed between 2017 and 2019—when cumulative damage reached approximately 270 million m^3—was also captured in alignment with G4M outputs. Beyond capturing the temporal trends, including the peak period, the model was evaluated against spatial disturbance patterns and known hotspots. It accurately reproduced major damage clusters in Central Europe, particularly in Germany and Poland, consistent with observed bark beetle outbreaks and windstorm paths during the reference period.

Dynamics of forest biomass

Forest growing stocks were obtained from the Global Forest Resources Assessment 2020 platform for the years 2000, 2010, and 2015 to 2020 (FAO, 2020). This data represents the stem volume of living trees, excluding branches. In general, stem carbon stock can be estimated as a function of growing stock volume by multiplying it by wood density (kg/m^3) and carbon content (tC/t), with each parameter assumed to be about 0.5 at the global level (IPCC, 2006; FAO, 2015).

The stem carbon stock was used to calibrate and validate the living stemwood biomass of G4M during the historical period (2000 to 2010). Next, the simulation for 2011 to 2020 was done without using the observations. A comparison of the model simulated output with actual data (FAO, 2020) aggregated over the study area is presented in Figure 12, showing that the trend provided by the integrated model achieved a strong fit with the data, with a slight underestimation towards the end of the historical period (2015–2020). This underestimation may be partly attributed to the lack of representation of selective salvage logging, which could have contributed to preserving more living biomass. Furthermore, the model assumed uniform reforestation with the same species throughout the historical period, whereas in reality, efforts to improve forest productivity may have been implemented. Nonetheless, the overall agreement is reasonably robust.

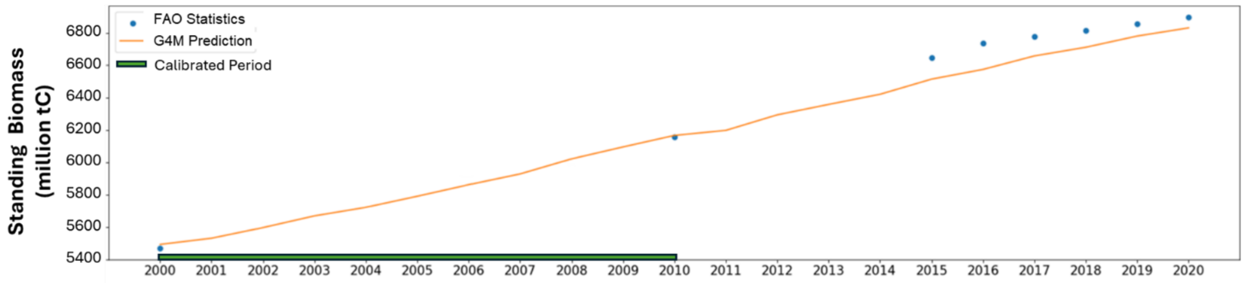

Figure 12: Yearly development of biomass in the EU-27 forest land modelled by G4M coupled with natural disturbances module and reported by FAO.

3.2. Simulation of scenarios during the projection period

Simulations of burned areas, bark beetle and windstorm damage, and living stem biomass, were conducted for three management scenarios, defined in Section 2.8, and were paired with two climate change scenarios corresponding to two global warming levels. Here, we present the aggregated values for the scenarios, while the following section will illustrate the spatial distribution of their impacts on forests and natural disturbances.

Conservation Scenario

Simulated burned areas for the conservation scenario are presented in Figure 13. The figure illustrates increasing trends of burned areas for the two global warming levels. Notably, the model projects extreme events between 2030–2040 and 2050–2060. In addition to more stochastic peaks, the GWL3 (consistent with RCP 8.5) projected a higher increase in burned areas compared to the GWL2 scenario (consistent with RCP 4.5). Detailed average values for projected burned areas and forest biomass, along with comparisons to the historical period, are provided in Table .4 compares the historical 20-year average (2001–2020) with two future periods, 2031–2050 and 2051–2070. Burned areas increase in future periods under both climate scenarios.

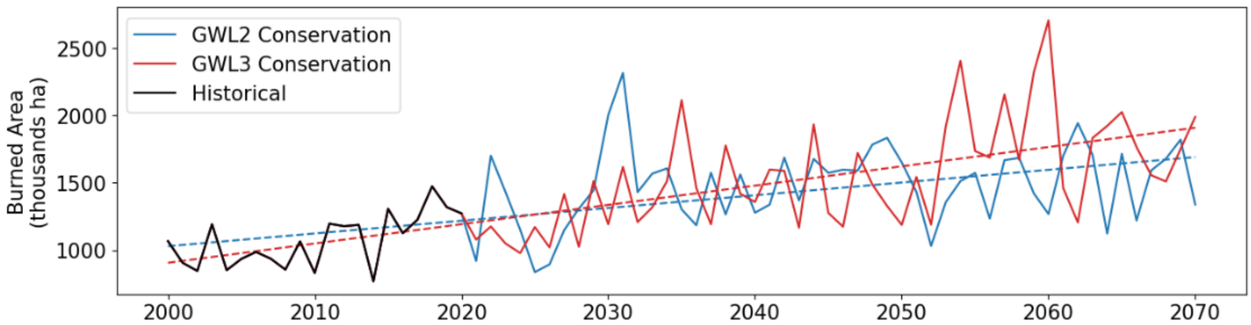

Figure 13: Simulated burned areas in forest, shrubland, cropland, and grassland in the EU-27 under the conservation scenario and two climate change scenarios.

Simulated bark beetle and windstorm damage are illustrated in Figure 14, showing considerable stochastic peaks between 2025 and 2045 and a decreasing trend toward 2070. This is explained by post-disturbance management, which promotes planting broadleaf species in the conservation scenario, which gradually reduces the risk of windstorm and beetles damage over time. The associated transition from coniferous to broadleaf species is illustrated in Figure 15, which illustrates a rapid decline in coniferous forest area. However, the trend in coniferous area does not fully align with the trend in disturbance, as bark beetle and windstorm impacts are also heavily influenced by climatic factors such as wind gust intensity. Additionally, not only forest area but also age structure plays a crucial role: younger forests with lower spruce basal area are less susceptible to bark beetle outbreaks. As a result, the GWL3 scenario, despite having lower overall conifer (spruce) abundance, exhibits greater disturbance due to the amplified impacts of climate change.

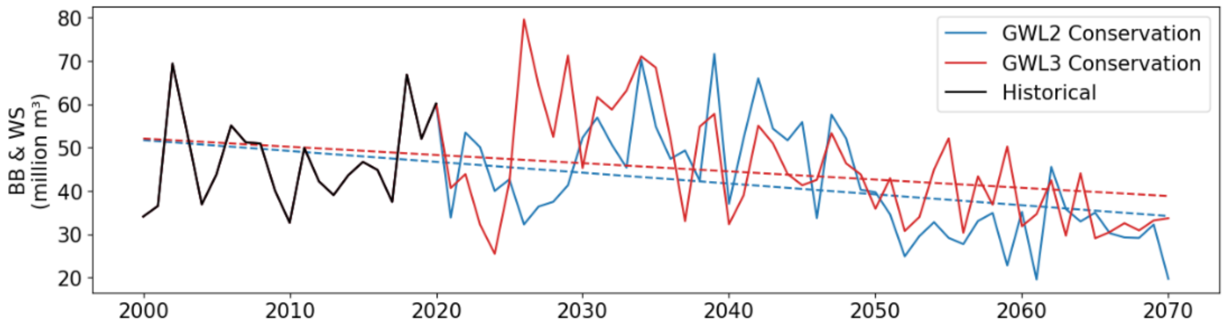

Figure 14: Simulated bark beetle and windstorm damage in the EU-27 forest land under the conservation scenario and two climate change scenarios.

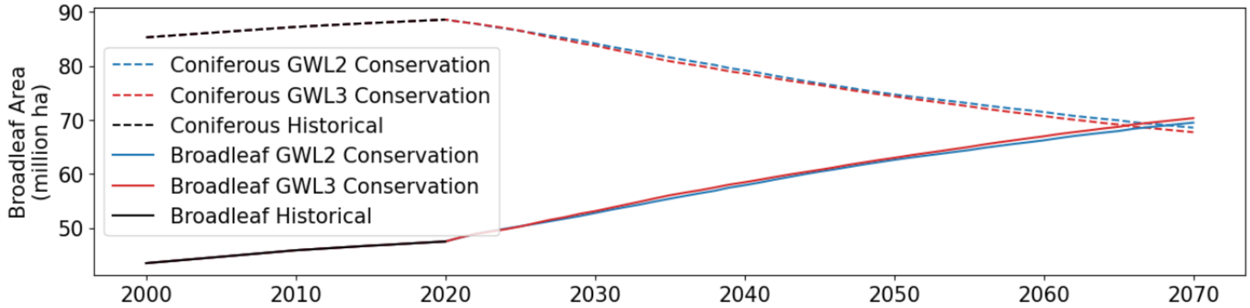

Figure 15: Projected forest area by type (Broadleaf and Coniferous) in the EU-27 under the conservation scenario and two climate change scenarios.

The annual dynamics of living stem biomass in forests, corresponding to disturbances, are shown in Figure 16. The Figure illustrates that the conservation scenario supports a steady increase in biomass across the study area, extending trends initialized during the historical period (as shown in Figure 12). However, biomass levels under the GWL3 scenario are slightly lower than those under GWL2. Average values are summarized in Table 4.

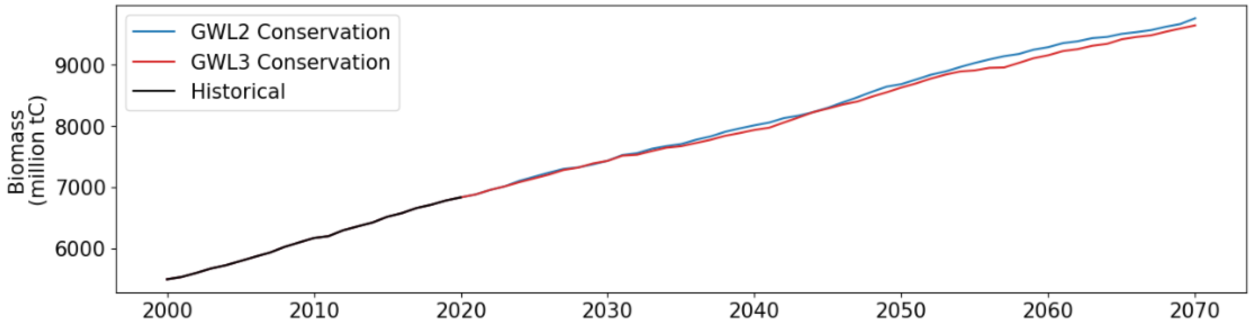

Figure 16: Projected development of future living stem biomass in the EU-27 forest land under the conservation scenario and two climate change scenarios.

Table 4: Average annual burned area, biomass, and bark beetle and windstorm damage in EU-27 modeled by FLAM, G4M, and PICUS for the conservation scenario of two future projection periods compared to the historical period. Global Warming Level 2 and 3 correspond to RCP scenarios 4.5 and 8. Burned area is reported in thousands of hectares, Biomass in million tC, and Bark beetle and windstorm damage in million m³.

Time Period	Type	Burned Area (thousands ha)		Bark Beetle & Windstorm Damage (million m³)		Living Stem Biomass (million tC)	
	Scenario	GWL2	GWL3	GWL2	GWL3	GWL2	GWL3
Historical (2001–2020)	Annual Average	1072.05 ± 195.76		47.61 ± 9.76		6186.34 ± 402.43	
Future (2031–2050)	Annual Average	1558.24 ± 246.24	1470.71 ± 258.92	51.44 ± 10.02	50.24 ± 11.04	8055.06 ± 355.32	8005.86 ± 345.77
	Δ Annual Average	+ 486.19	+ 398.66	+ 3.83	+ 2.63	+ 1868.72	+ 1819.52
Future (2051–2070)	Annual Average	1499.76 ± 240.48	1816.03 ± 372.69	30.67 ± 5.89	36.87 ± 7.03	9280.07 ± 284.01	9173.58 ± 281.93
	Δ Annual Average	+ 427.71	+ 743.98	- 16.94	- 10.74	+ 3093.73	+ 2987.24

Source: ForestNavigator WP 3, standard deviations are reported

The integrated model enables the assessment of disturbance-related damages in terms of carbon loss. Figure 17 presents the annual values of accumulated harvest, changes in stem wood biomass, and losses from bark beetle, wind, and wildfire for both global warming levels.

In our assessment, harvest is considered to be a positive factor in computing the cumulative carbon sequestration, herein we assume that harvested biomass is fully allocated to carbon storage with indefinite duration, which may not accurately reflect real-world carbon dynamics. Oppositely, disturbances are considered only as biomass loss and did not account for wood recover from salvage logging (i.e., windstorms or bark beetle outbreaks), which can be partially recovered. Nevertheless, we believe this accounting approach effectively highlights the long-term quantitative differences between our stylized management scenarios.

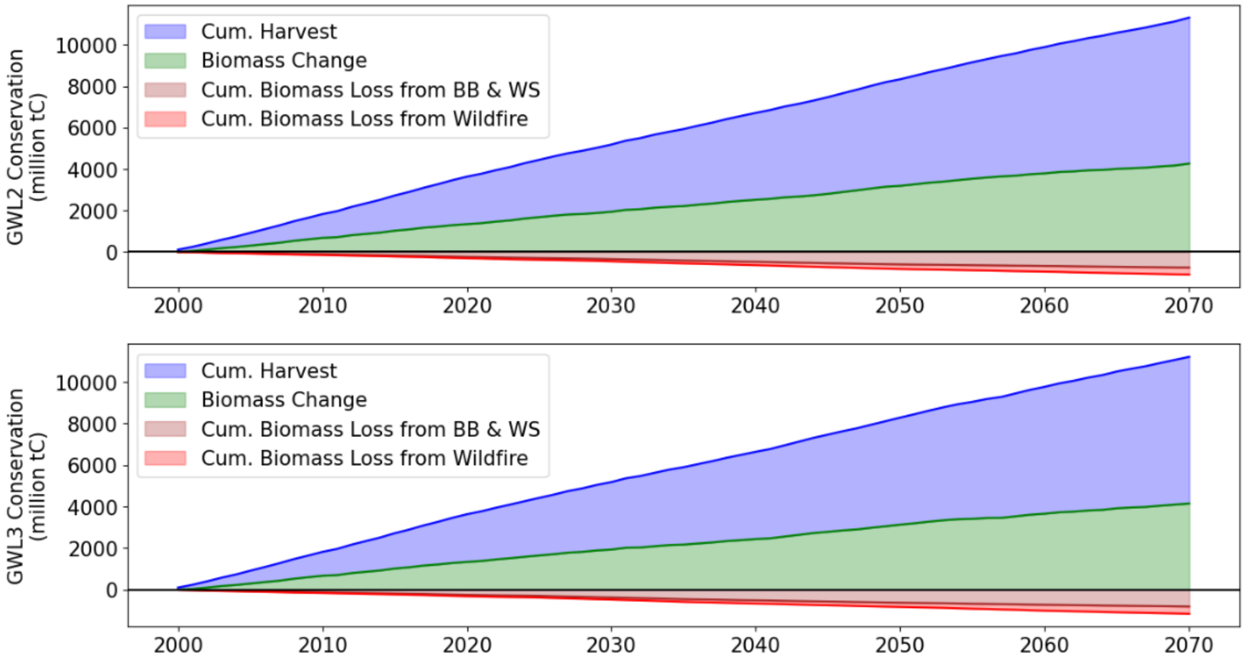

Figure 17: Projected cumulative biomass gains and losses from 2000 to 2070 for EU-27 forest land under the conservation scenario across two climate change scenarios.

To calculate net carbon sequestration, cumulative biomass gains and losses are aggregated to 10-year intervals in Table 5.

According to our carbon quantification approach, under the GWL2 scenario we observe a higher net carbon sequestration and lower biomass loss compared to GWL3.

The spatial transition will be illustrated in the following section, demonstrating that despite minor changes at the aggregate level, there are significant regional differences across Europe in response to the management scenarios.

Table 5: Projected cumulative biomass gains, disturbance-related losses, and net carbon sequestration (defined as the sum of cumulated harvest and living stem biomass gain) for EU-27 forest land in million tC from 2000 under the conservation scenario across two climate change scenarios.

Time Period	Living Stem Biomass Gain (million tC)		Biomass Loss from Disturbances (million tC)		Net Carbon Sequestration (million tC)	
	GWL2	GWL3	GWL2	GWL3	GWL2	GWL3
2020	1337.00		314.13		3629.89	
2030	1935.19	1932.66	461.44	474.05	5180.25	5177.72
2040	2513.63	2437.98	646.60	663.90	6710.87	6635.23
2050	3185.91	3130.67	832.73	827.44	8335.34	8280.10
2060	3789.31	3657.29	961.00	1008.46	9890.91	9758.89
2070	4261.85	4145.36	1100.81	1158.65	11315.63	11199.15

Economic Scenario

Simulated burned areas for the economic scenario are presented in Figure 18. The figure illustrates increasing trends of burned areas under global warming levels. Notably, the model projects extreme events between 2030–2040 and 2050–2060. In addition to more stochastic peaks, GWL3 (consistent with RCP 8.5) projected a higher increase in burned areas compared to the GWL2 scenario (consistent with RCP 4.5). Detailed average values for projected burned areas and forest biomass, along with comparisons to the historical period, are provided in Table 6. The increase in burned areas is slightly larger than in the conservation scenario under both global warming levels, since in the economic scenarios, the most productive species are planted and there is no increase in broadleaved species. However, under this stochastic realization, the graphs for the conservation and economic scenarios appear visually identical. Based on the table, the difference in the first future period seems very small, especially when considering the standard deviation. Despite similar aggregate numbers, the scenarios show notable spatial differences, which are presented in the next section.

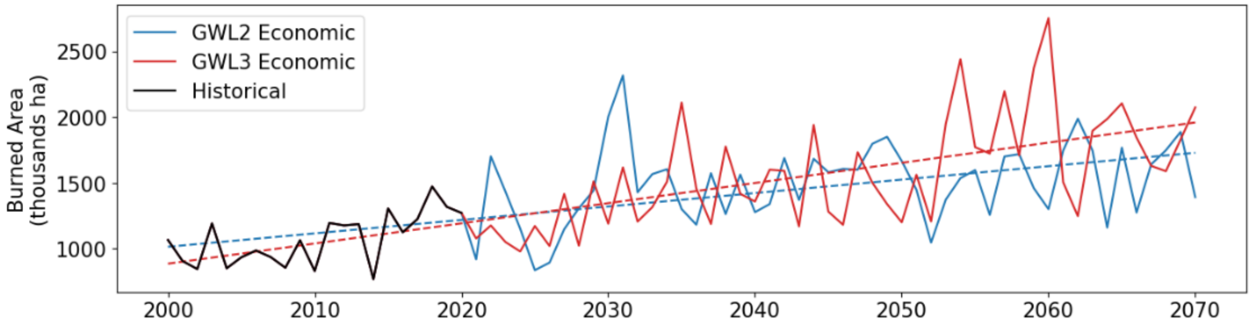

Figure 18: Simulated burned areas for EU-27 under the economic scenario and two climate change scenarios.

Simulated bark beetle and windstorm damage are illustrated in Figure 19, showing considerable stochastic peaks between 2025 and 2045, and toward the end of the second future period. While the GWL2 scenario demonstrates a decreasing trend toward 2070, in the GWL3 scenario, the trend slightly increases over time. Comparing this figure with Figure 14, one can see that the main difference occurs during the 2060–2070 period, where this scenario under GWL3 results in higher peaks than the conservation scenario. This is primarily due to the slower transition to broadleaf species in the economic scenario, as illustrated in Figure 20. Unlike the conservation scenario, where coniferous forest area declines rapidly, the reduction under the economic scenario is more gradual, thereby maintaining greater susceptibility to bark beetle and windstorm.

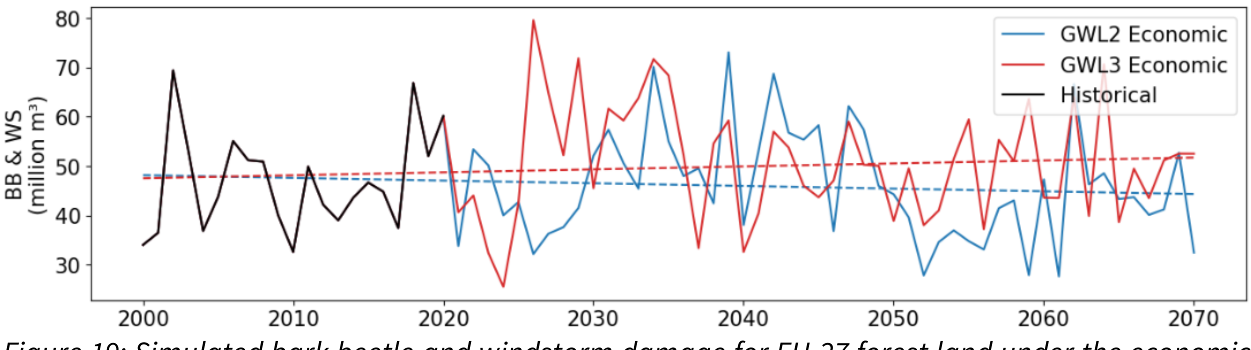

Figure 19: Simulated bark beetle and windstorm damage for EU-27 forest land under the economic scenario and two climate change scenarios.

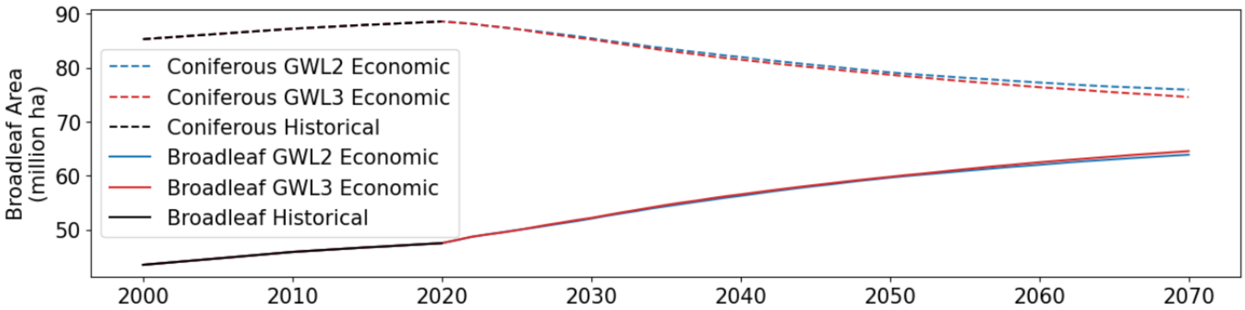

Figure 20: Projected forest area by type (Broadleaf and Coniferous) under the economic scenario and two climate change scenarios for EU-27

The annual dynamics of living stem biomass in forests, corresponding to disturbances, are shown in Figure 21. The figure shows that the economic scenario supports an increase in biomass across the study area, similar to the conservation scenario. Under the GWL3 scenario, biomass levels are slightly lower than those under GWL2. Average values for the economic scenario are summarized in Table 6. We observe that living stem biomass gains are slightly higher in the conservation scenario until 2060. However, by 2070, the economic scenario results in higher values. The burned area follows a similar trend in both scenarios, while bark beetle and windstorm-related volumes appear to increase significantly under the economic scenario. Due to the assumption of indefinite carbon storage in harvested wood, the potential net carbon sequestration is also higher in the economic scenario.

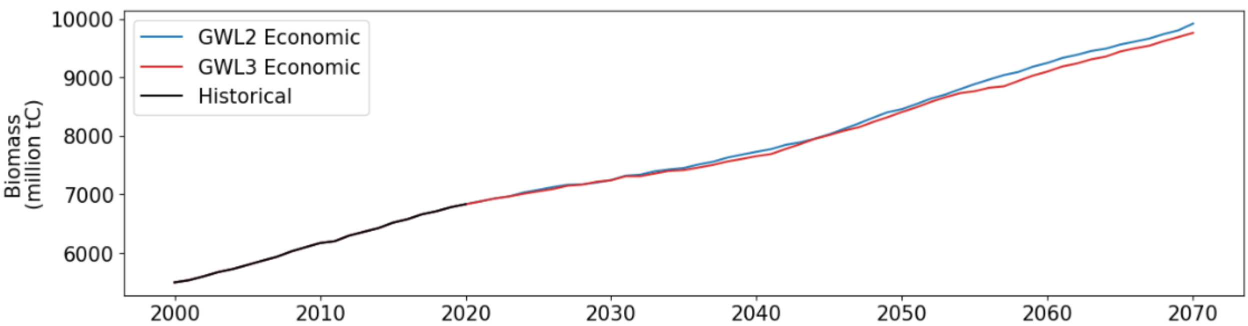

Figure 21: Projected development of future living stem biomass for EU-27 forest land under the economic scenario and two climate change scenarios

Table 6: Economic scenario. Average annual burned area, biomass, and bark beetle and windstorm modeled by FLAM, G4M, and PICUS for EU-27 for the economic scenario in 2 future projection periods, and as compared to historical average. Global Warming Level 2 and 3 correspond to RCP scenarios 4.5 and 8. Burned area is reported in thousands of hectares, Biomass in million tC, and Bark beetle and windstorm damage in million m^3.

Time Period	Type	Burned Area (thousands ha)		Bark Beetle & Windstorm Damage (million m^3)		Living Stem Biomass (million tC)	
	Scenario	GWL2	GWL3	GWL2	GWL3	GWL2	GWL3
Historical (2001–2020)	Annual Average	1072.05 ± 195.76		47.61 ± 9.76		6186.34 ± 402.43	
Future	Annual Average	1562.91 ± 249.28	1474.70 ± 258.79	53.41 ± 9.82	52.14 ± 10.58	7800.25 ± 351.83	7752.32 ± 344.91

Time Period	Type	Burned Area (thousands ha)		Bark Beetle & Windstorm Damage (million m³)		Living Stem Biomass (million tC)	
	Scenario	GWL2	GWL3	GWL2	GWL3	GWL2	GWL3
(2031–2050)							
	Δ Annual Average	+ 490.85	+ 402.65	+ 5.80	+ 4.53	+ 1613.91	+ 1565.98
Future (2051–2070)	Annual Average	1539.34 ± 248.30	1869.36 ± 376.40	40.46 ± 9.17	49.79 ± 9.16	9252.86 ± 398.53	9130.13 ± 380.58
	Δ Annual Average	+ 467.29	+ 797.31	- 7.14	+ 2.19	+ 3066.51	+ 2943.79

The carbon assessment for economic scenario is given in Figure 22. Due to more intensive harvest, harvested carbon is considerably higher than in the conservation scenario.

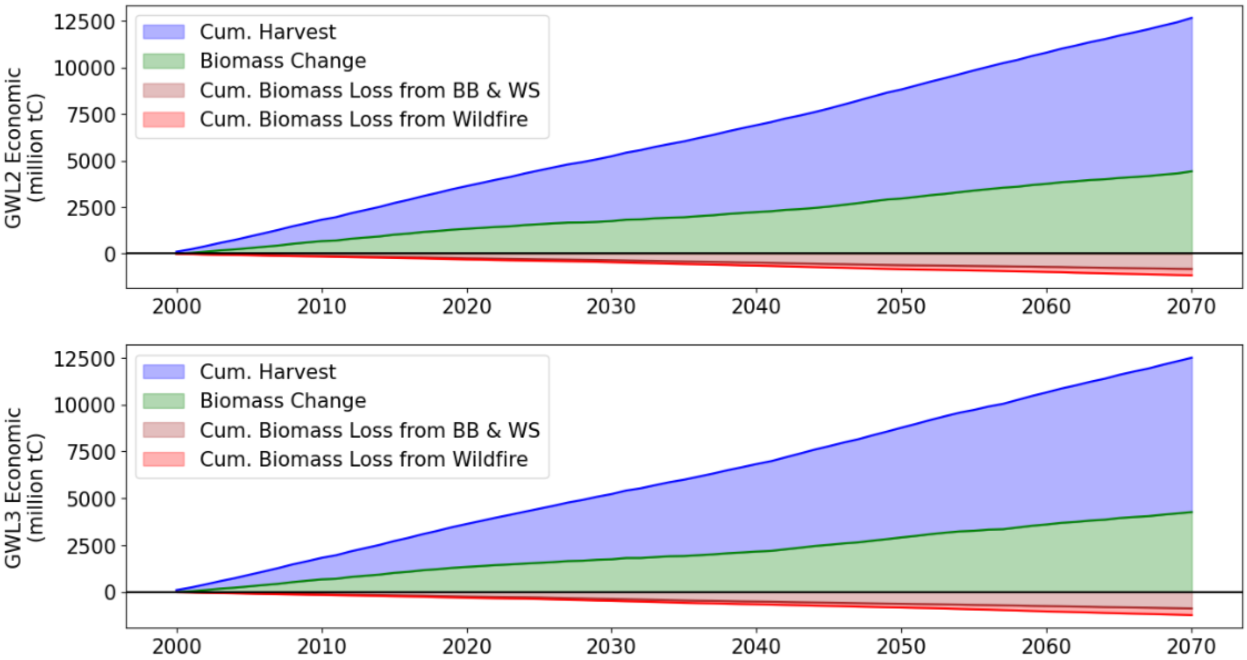

Figure 22: Projected cumulative biomass gains and losses from 2000 to 2070 for EU-27 forest land under the economic scenario across two climate change scenarios.

Projected changes in carbon sequestration are shown in Table 7. Compared to the conservation scenario, the economic scenario projects higher gains in net carbon sequestration due to larger harvest amounts despite higher losses from disturbances.

Table 7: Projected cumulative biomass gains, disturbance-related losses, and net carbon sequestration (defined as the sum of cumulated harvest and living stem biomass gain) for EU-27 forest land in million tC from 2000 under the economic scenario across two climate change scenarios.

Time Period	Living Stem Biomass Gain (million tC)		Biomass Loss from Disturbances (million tC)		Net Carbon Sequestration (million tC)	
	GWL2	GWL3	GWL2	GWL3	GWL2	GWL3
2020	1337.00		314.13		3629.89	
2030	1749.41	1745.67	460.81	473.94	5232.52	5228.79
2040	2233.60	2158.98	645.17	662.96	6906.93	6832.31
2050	2962.86	2914.56	839.31	834.18	8826.42	8778.12
2060	3752.97	3605.71	984.84	1041.23	10806.76	10659.5
2070	4426.13	4267.36	1163.84	1238.61	12670.14	12511.36

Societal Scenario

Simulated burned areas, damages from bark beetle and windstorm disturbances and development of living stem biomass for the societal scenario are presented in Figure 23, Figure 24, Figure 26. Figures show increasing trends for burned areas with higher levels under GWL3, and increasing trends in two other disturbances with higher decrease under GWL2. Projected stem biomass is similar to conservation scenario but below the economic scenario. As illustrated in Figure 25, the transition to broadleaf species in terms of forest area occurs at an intermediate pace in the societal scenario—slower than in the conservation scenario but faster than in the economic one. However, due to a higher harvest target compared to the conservation scenario, the transition to broadleaf species in terms of forest biomass is accelerated. As a result, spruce basal area declines more rapidly, leading to a corresponding reduction in bark beetle and windstorm damage. This decline in disturbance is further reinforced by the societal scenario's generally lower baseline levels of living stem biomass, which contribute to reduced vulnerability.

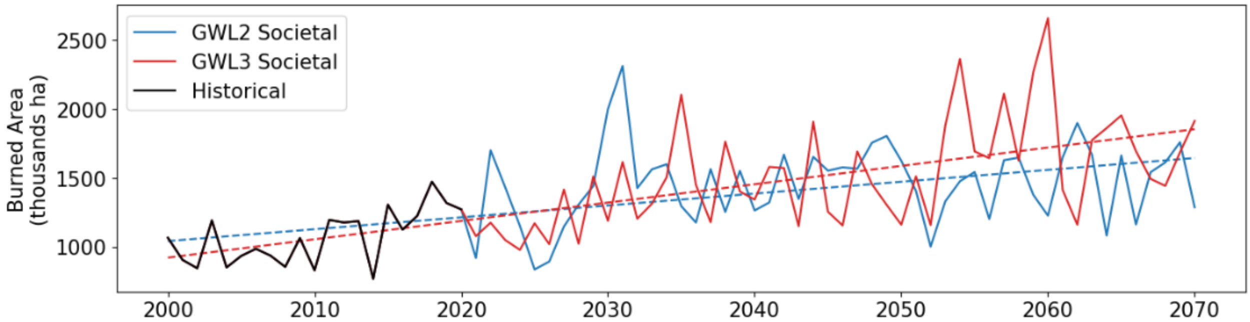

Figure 23: Simulated burned areas for EU-27 under the societal scenario and two climate change scenarios.

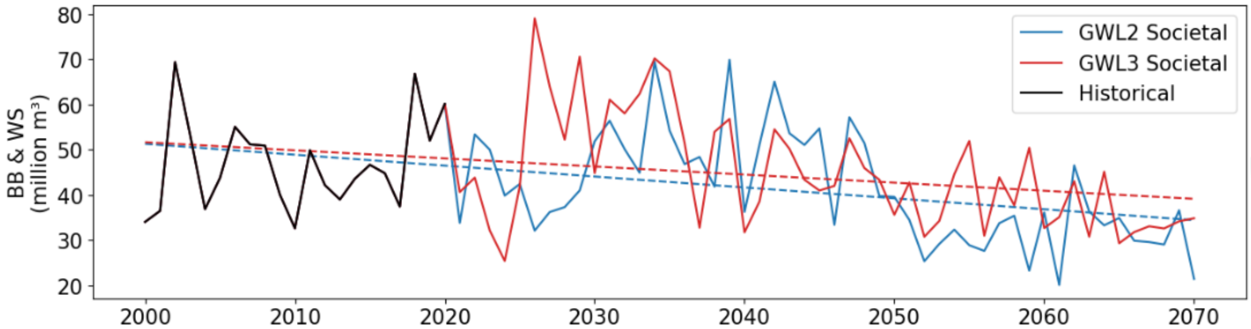

Figure 24: Simulated bark beetle and windstorm damage for EU-27 forest land under the societal scenario and two climate change scenarios.

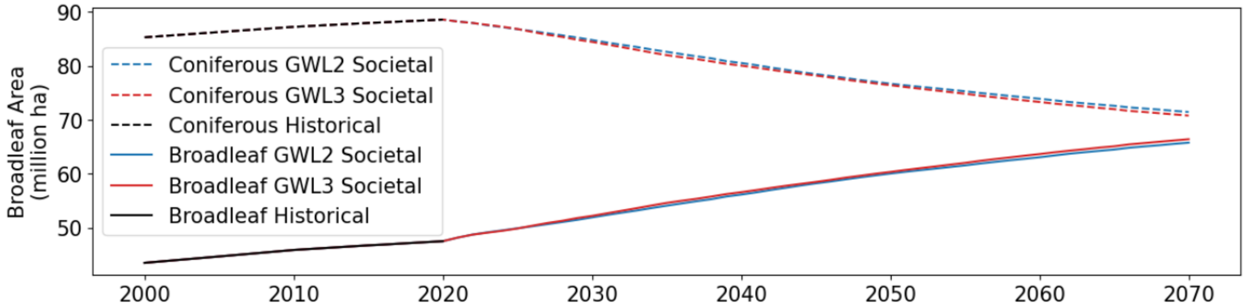

Figure 25: Projected forest area for EU-27 by type (Broadleaf and Coniferous) under the societal scenario and two climate change scenarios

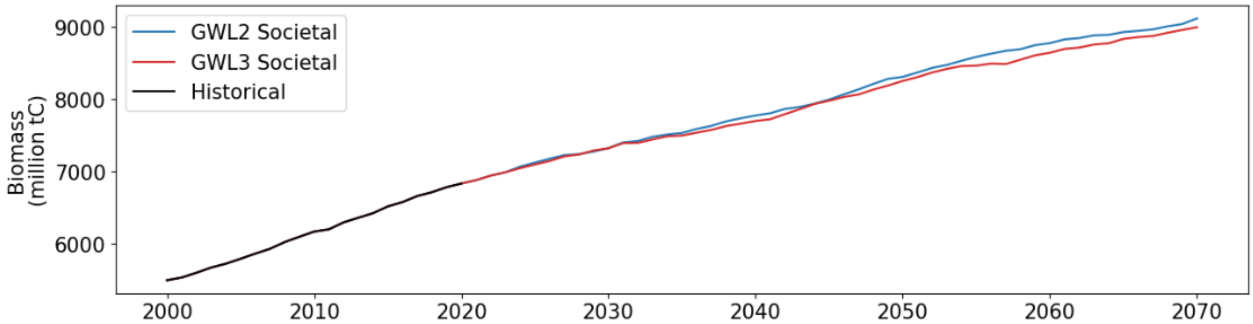

Figure 26: Projected development of future living stem biomass for EU-27 forest land under the societal scenario and two climate change scenarios.

Averaged values for future intervals are shown in Table 8. The societal scenario leads to less burned areas compared to the conservation and economic scenarios, the damage from bark beetle and windstorms is like conservation scenarios. However, the increase in living stem biomass is the lowest in the societal scenario.

Table 8: Societal scenario. Average annual burned area, biomass, and bark beetle and windstorm modeled by FLAM, G4M, and PICUS for each scenario in 2 future projection periods, and as compared to historical average. Global Warming Level 2 and 3 correspond to RCP scenarios 4.5 and 8. Burned area is reported in thousands of hectares, Biomass in million tC, and Bark beetle and windstorm damage in million m^3.

Time Period	Type	Burned Area (thousands ha)		Bark Beetle & Windstorm Damage (million m^3)		Living Stem Biomass (million tC)	
	Scenario	GWL2	GWL3	GWL2	GWL3	GWL2	GWL3
Historical (2001–2020)	Annual Average	1072.05 ± 195.76		47.61 ± 9.76		6186.34 ± 402.43	
Future (2031–2050)	Annual Average	1543.77 ± 245.37	1455.31 ± 259.02	50.77 ± 9.81	49.64 ± 10.85	7810.49 ± 278.89	7760.93 ± 268.96
	Δ Annual Average	+ 471.71	+ 383.26	+ 3.16	+ 2.03	+ 1624.14	+ 1574.58
Future (2051–2070)	Annual Average	1458.03 ± 236.88	1765.08 ± 371.55	31.21 ± 5.99	37.49 ± 6.77	8764.00 ± 208.34	8654.73 ± 203.77
	Δ Annual Average	+ 385.97	+ 693.02	- 16.4	- 10.12	+ 2577.66	+ 2468.39

The carbon estimation for societal scenario shown in Figure 27 and summarized in Table 9 show that it is relatively close to conservation scenario, but projects less biomass gain and less loss from disturbances. However, the carbon sequestration values are lowest in this scenario compared to economic and conservation scenarios.

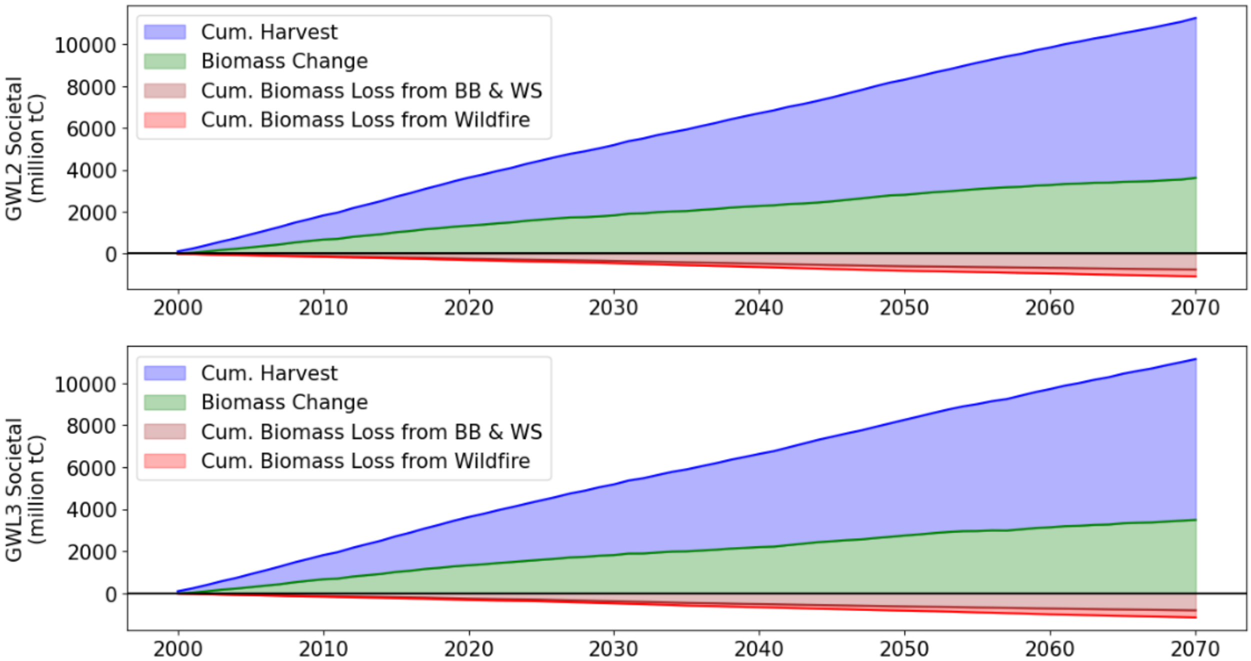

Figure 27: Projected cumulative biomass gains and losses from 2000 to 2070 for EU-27 forest land under the societal scenario across two climate change scenarios.

Table 9: Projected cumulative biomass gains, disturbance-related losses, and net carbon sequestration (defined as the sum of cumulated harvest and living stem biomass gain) for EU-27 forest land in million tC from 2000 under the societal scenario across two climate change scenarios.

Time Period	Living Stem Biomass Gain (million tC)		Biomass Loss from Disturbances (million tC)		Net Carbon Sequestration (million tC)	
	GWL2	GWL3	GWL2	GWL3	GWL2	GWL3
2020	1337.00		314.13		3629.89	
2030	1826.62	1823.84	460.79	473.20	5190.71	5187.93
2040	2277.32	2202.19	643.02	660.06	6712.61	6637.48
2050	2811.88	2755.45	825.25	820.41	8318.37	8261.94
2060	3278.34	3144.57	951.29	997.88	9856.03	9722.27
2070	3619.77	3498.05	1089.17	1146.04	11268.66	11146.95

3.3. Comparing the spatial pattern of biomass by scenario transition

In this section, we analyze the interplay between various management scenarios and global warming, assessing the impact of transitioning from one scenario to another. This approach captures the effects of forest management on future forest dynamics, carbon sequestration potential, and exposure to natural disturbances under climate change conditions. Across all management and climate change scenarios, the overall patterns of living biomass change, harvested biomass, and disturbance-related biomass loss showed relatively minor differences in absolute values. This consistency is primarily due to a shared baseline in forest age structure, species composition, and regional growth potential.

Widespread biomass stock increment was observed across Europe, with particularly notable increases in Western and Southern Europe, including regions corresponding to present-day France, Italy, and Eastern Central Europe (e.g., Poland). Both harvest and disturbance hotspots were concentrated in Central and Southeastern Europe, including parts of the Iberian Peninsula and the Balkan region.
While the absolute values remained similar, the differences between scenarios became more apparent when examining the spatial deltas(Δ), highlighting where and how management strategies and climate pathways diverge in their impacts.

Comparison of forest management scenarios

Figure 28 illustrates the spatial changes after transitioning from the conservation scenario (top figure) to the economic scenario (bottom figure) and vice versa. The following color scheme is used: Red (disturbance-related loss), Green (Biomass gain), Blue (Harvest).

Transition from economic to conservation scenario

In case of transition from the economic to conservation scenario (left figure), we observe increasing disturbances (red) in Central Europe, due to higher fuel loads because of the reduced forestry intervention and accumulation of biomass. Biomass gain (green) increases widely across Europe, especially in Scandinavia, which is driven by reduced harvest pressure and extended rotation periods. The harvest (blue) significantly decreases across most regions, reflecting a shift to lower harvest intensity under conservation management.

Transition from conservation to economic scenario

Disturbance Loss (red) increases in Scandinavia and parts of Central Europe, where spruce-dominated forests are maintained, making them more susceptible to bark beetle outbreaks and windthrow. Biomass gain (green) increases in Central Europe due to management practices that promote and maintain a productive age structure. Harvest (blue) increases widely across Europe, reflecting intensified forest use under the economic management scenario.

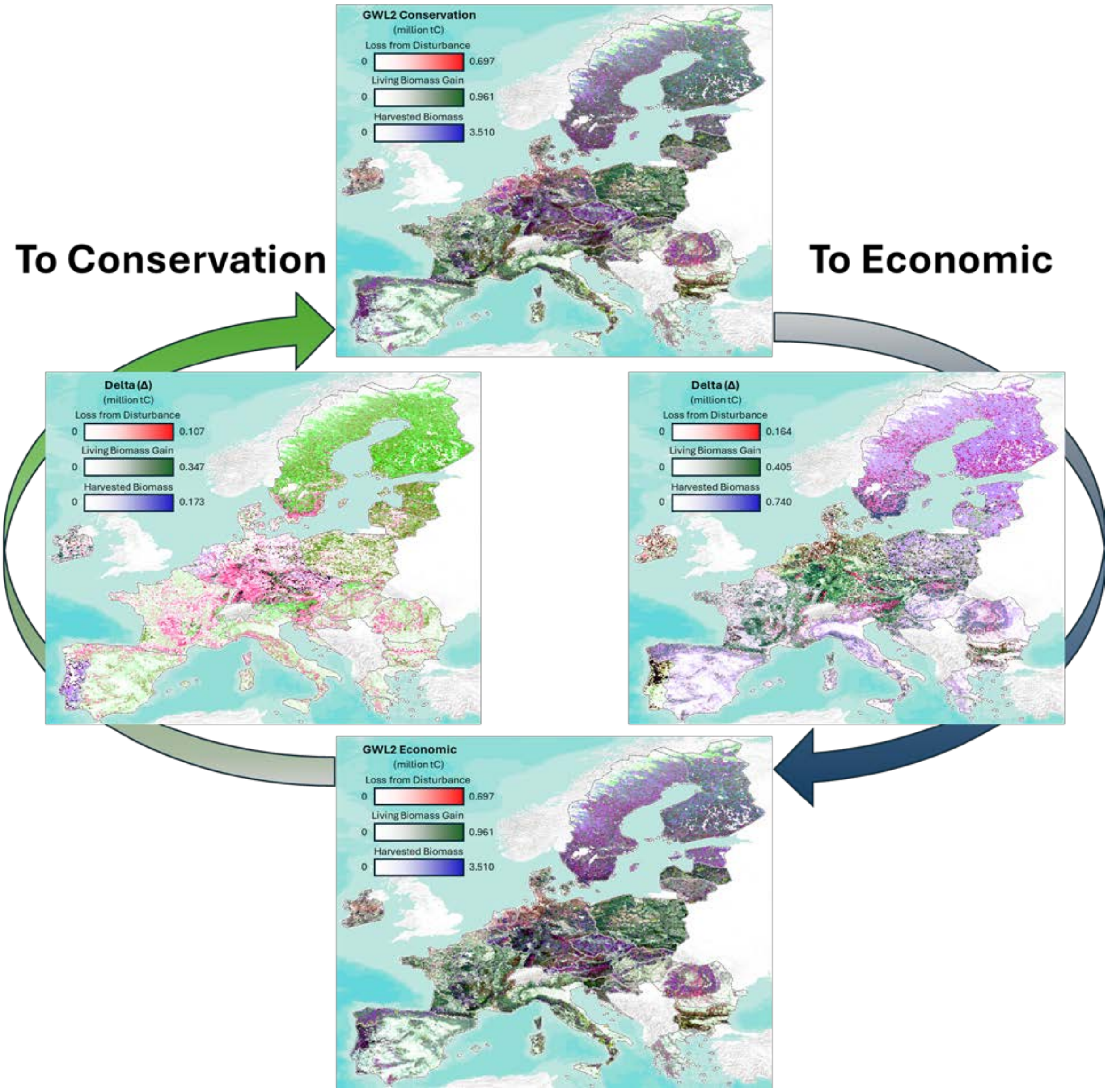

Figure 28: Projected spatial changes in biomass gain, harvest, and disturbance under GWL2 climate across conservation and economic management scenarios for EU-27 forest land

Comparison of climate change scenarios

Differences between the GWL2 (top figure) and GWL3 (bottom figure) scenarios are shown in Figure 29.

Cooling transition from GLW3 to GLW2

Under a cooler climate (left figure), biomass increases widely across Europe (green), especially in Iberia and Central Europe, as reduced climate stress enhances forest productivity. Under the GWL2 scenario, disturbance hotspots (red) do not shift further north as they do under GWL3. Instead, they remain in their current locations, leading to relatively higher disturbance activity in Central Europe compared to GWL3.

Warming Transition from GLW2 to GLW3

Under a hotter climate (right figure), combined disturbances (red) increase, driven by the heightened risk of wildfires, windstorms, and bark beetle outbreaks. Biomass gain (green) occurs primarily in high-altitude areas and parts of Central Europe, where warming may temporarily enhance growth conditions. However, in Central Europe, areas of biomass gain and disturbance increase spatially overlap, suggesting that while forests may continue to grow, they are also increasingly vulnerable to climate-driven disturbances—highlighting a growing instability in forest carbon dynamics under high warming scenarios.

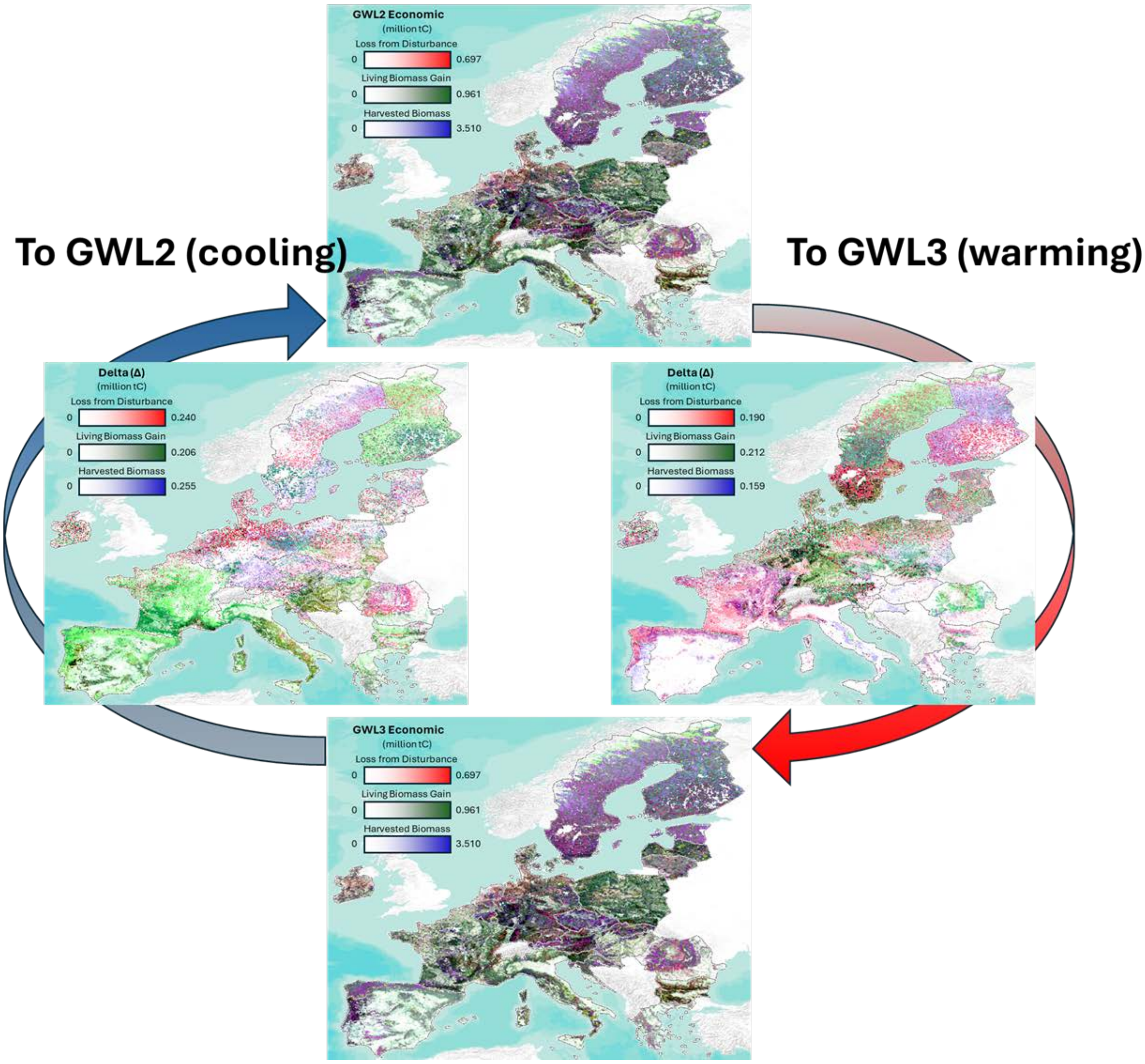

Figure 29: Projected spatial changes in biomass gain, harvest, and disturbance under warming and cooling transitions in the economic scenario for EU-27 forest land

4. Conclusion

The results presented in this deliverable demonstrate that forest management choices have a profound impact on future forest dynamics, carbon sequestration potential, and the exposure to natural disturbances under climate change. The integrated modeling approach developed here enables a nuanced assessment of these trade-offs, providing key insights for the ForestNavigator project's goal of supporting evidence-based, climate-resilient forest policy across Europe.

These early findings reinforce the need for differentiated strategies that balance productivity with resilience. While intensive management can enhance carbon uptake through increased harvesting, it may also increase the risk of bark beetle outbreaks and windstorms in Northern and parts of Central Europe under future climate scenarios, due to the continued dominance of coniferous species. In contrast, more conservation-oriented strategies result in lower disturbance impacts from bark beetles and windstorms in Northern Europe. However, they can lead to higher fire disturbances in Central and Southern Europe due to fuel accumulation from reduced harvesting. The societal scenario resulted in the lowest combined damage from disturbances. This could be explained by a greater proportion of broadleaf planting compared to the economic scenario and a higher level of harvesting than in the conservation scenario. Consequently, the transition to broadleaves may proceed more quickly than in the conservation scenario, along with reduced fuel accumulation. However, this benefit comes at the cost of the lowest standing biomass. Therefore, the new model can help to identify optimal mixes and regional priorities for forest adaptation and mitigation planning.

This deliverable significantly contributes to the project's impact by offering a tool that supports scenario analysis at the EU level and enables further spatially explicit assessments at national and sub-national levels. The modeling framework is now ready to be integrated into ongoing and upcoming policy-relevant simulations conducted by other ForestNavigator partners, including those focused on land-use dynamics, biodiversity, and socioeconomic outcomes.

In the next phase, the modeling outputs will be refined through stakeholder feedback and used to inform policy pathways**,** regional case studies, and sectoral dialogues**.** Future work will focus on coupling this forest model with broader land-use and economic models, ensuring consistency across policy-relevant dimensions.

5. References

Arellano-del-Verbo, G., Urbieta, I. R., & Moreno, J. M. (2023). Large-fire ignitions are higher in protected areas than outside them in West-Central Spain. *Fire*, 6(1), 28. https://doi.org/10.3390/fire6010028.

Arora, V. K., & Boer, G. J. (2005). Fire as an interactive component of dynamic vegetation models. Journal of Geophysical Research: *Biogeosciences*, 110(G2). https://doi.org/10.1029/2005JG000042. https://doi.org/10.1029/2005JG000042

Berčák, R., Holuša, J., Kaczmarowski, J., Tyburski, Ł., Szczygieł, R., Held, A., ... & Chromek, I. (2023). Fire protection principles and recommendations in disturbed forest areas in central europe: a review. *Fire*, 6(8), 310. https://doi.org/10.3390/fire6080310

Buchhorn, M., Lesiv, M., Tsendbazar, N. E., Herold, M., Bertels, L., & Smets, B. (2020). Copernicus global land cover layers—collection 2. *Remote Sensing*, 12(6), 1044. https://doi.org/10.3390/rs12061044.

Chen, Y., Hall, J., Van Wees, D., Andela, N., Hantson, S., Giglio, L., ... & Randerson, J. T. (2023). Multi-decadal trends and variability in burned area from the 5th version of the Global Fire Emissions Database (GFED5). *Earth System Science Data Discussions,* 2023, 1-52. https://doi.org/10.5194/essd-15-5227-2023.

Chuvieco, E., Lizundia-Loiola, J., Pettinari, M. L., Ramo, R., Padilla, M., Tansey, K., ... & Plummer, S. (2018). Generation and analysis of a new global burned area product based on MODIS 250 m reflectance bands and thermal anomalies. *Earth System Science Data*, 10(4), 2015-2031. https://doi.org/10.5194/essd-10-2015-2018.

Chuvieco, E., Pettinari, M. L., Lizundia Loiola, J., Storm, T., & Padilla Parellada, M. (2019). ESA Fire Climate Change Initiative (Fire_cci): MODIS Fire_cci Burned Area Grid product, version 5.1. https://doi.org/10.5285/3628cb2fdba443588155e15dee8e5352.

Corning, S., Krasovskiy, A., Kiparisov, P., San Pedro, J., Viana, C. M., & Kraxner, F. (2024). Anticipating future risks of climate-driven wildfires in boreal forests. *Fire*, 7(4), 144. https://doi.org/10.3390/fire7040144.

Cunningham, C. X., Williamson, G. J., & Bowman, D. M. (2024). Increasing frequency and intensity of the most extreme wildfires on Earth. *Nature ecology & evolution*, 8(8), 1420-1425. https://doi.org/10.1038/s41559-024-02452-2. https://doi.org/ 10.1038/s41559-024-02452-2

European Commission (EC). (2013). COMMUNICATION FROM THE COMMISSION TO THE EUROPEAN PARLIAMENT, THE COUNCIL, THE EUROPEAN ECONOMIC AND SOCIAL COMMITTEE AND THE COMMITTEE OF THE REGIONS: Green Infrastructure (GI) - Enhancing Europe's Natural Capital (No. COM/2013/0249 final). Publications Office of the European Union.

European Commission (EC). (2020). COMMUNICATION FROM THE COMMISSION TO THE EUROPEAN PARLIAMENT, THE COUNCIL, THE EUROPEAN ECONOMIC AND SOCIAL COMMITTEE

AND THE COMMITTEE OF THE REGIONS: EU Biodiversity Strategy for 2030 - Bringing nature back into our lives (No. COM/2020/380 final). Publications Office of the European Union.

European Commission (EC). (2023). European Union Disaster Resilient Goals. Publications Office of the European Union.

European Commission (EC). (2024). Regulation (EU) 2024/1991 of the European Parliament and of the Council of 24 June 2024 on nature restoration and amending Regulation (EU) 2022/869.

Larjavaara, M., Brotons, L., Corticeiro, S., Espelta, J. M., Gazzard, R., Leverkus, A., Lovric, N., Maia, P., Sanders, T., Svoboda, M., Thomaes, A., & Vandekerkhove, K. (2023). Deadwood and fire risk in Europe. Publications Office of the European Union. https://doi.org/10.2760/553875.

Lauerwald, R., Dinh, L.-A., Balkovic, J., Doelman, J., Gusti, M., Di Fulvio, F. & Lessa-Derci-Augustynczik, A., 2023. D5.1 Response functions for forest and agricultural ecosystem services, carbon storage and GHG fluxes. LAMASUS Project Deliverable. Available at: https://www.lamasus.eu/wp-content/uploads/LAMASUS_D5.1_Response-functions.pdf [Accessed 10 April 2025].

Lexer, M. J., Hönninger, K. (1998): Simulated effects of bark beetle infestations on stand dynamics in *Picea abies* stands: Coupling a patch model and a stand risk model. In: Beniston, M., Innes, J. L. (eds.): *The impacts of climate variability on forests.* Lecture Notes In Earth Sciences 74, 329-338, Springer Verlag.

European Environment Agency. (2024). European climate risk assessment: executive summary. Publications Office of the European Union, Luxembourg. https://doi.org/10.2800/204249.

Food and Agriculture Organization (FAO). (2015). Global Forest Resources Assessment 2015: How are the World's Forests Changing? Food and Agriculture Organization of the United Nations, Rome.

Food and Agriculture Organization (FAO). (2020). Forest Resources Assessment (FRA): Forest growing stock, biomass, and carbon.

Food and Agriculture Organization (FAO). (2024). Forest Product Statistics (FAOSTAT): Forestry Production and Trade.

Fernandes, P. M. (2013). Fire-smart management of forest landscapes in the Mediterranean basin under global change. *Landscape and Urban Planning*, 110, 175-182. https://doi.org/10.1016/j.landurbplan.2012.10.014.

Fernandez-Carrillo, A., Patočka, Z., Dobrovolný, L., Franco-Nieto, A., & Revilla-Romero, B. (2020). Monitoring bark beetle forest damage in Central Europe. A remote sensing approach validated with field data. *Remote Sensing*, 12(21), 3634. https://doi.org/10.3390/rs12213634.

Fernandez-Anez, N., Krasovskiy, A., Müller, M., Vacik, H., Baetens, J., Hukić, E., ... & Cerda, A. (2021). Current wildland fire patterns and challenges in Europe: A synthesis of national perspectives. *Air, Soil and Water Research*, 14, 11786221211028185. https://doi.org/10.1177/11786221211028185.

Fischer, G., Nachtergaele, F., Prieler, S., Van Velthuizen, H. T., Verelst, L., & Wiberg, D. (2008). Global agro-ecological zones assessment for agriculture (GAEZ 2008). IIASA, Laxenburg, Austria and FAO, Rome, Italy, 10.

Forzieri, G., Girardello, M., Ceccherini, G., Mauri, A., Spinoni, J., Beck, P., ... & Cescatti, A. (2020). Vulnerability of European forests to natural disturbances. *Publications Office of the European Union: Luxembourg.* https://doi.org/10.2760/736558 (online).

Hirsch, K., Kafka, V., Tymstra, C., McAlpine, R., Hawkes, B., Stegehuis, H., ... & Peck, K. (2001). Fire-smart forest management: a pragmatic approach to sustainable forest management in fire-dominated ecosystems. *The Forestry Chronicle*, 77(2), 357-363. https://doi.org/10.5558/tfc77357-2.

IPCC (Intergovernmental Panel on Climate Change). (2006). Guidelines for National Greenhouse Gas Inventories: Volume 4 Agriculture, Forestry and Other Land Use. https://www.ipcc-nggip.iges.or.jp/public/2006gl/vol4.html.

IUCN and UNEP-WCWC. (2022). Protected planet: The world database on protected areas (WDPA). Cambridge, UK: UNEP-WCMC and IUCN. www. protectedplanet. net.

Jacob, D., Petersen, J., Eggert, B., Alias, A., Christensen, O. B., Bouwer, L. M., ... & Yiou, P. (2014). EURO-CORDEX: new high-resolution climate change projections for European impact research. *Regional environmental change*, 14, 563-578. https://doi.org/10.1007/s10113-013-0499-2.

Jo, H. W., Krasovskiy, A., Hong, M., Corning, S., Kim, W., Kraxner, F., & Lee, W. K. (2023). Modeling historical and future forest fires in South Korea: The FLAM optimization approach. *Remote Sensing, 15(5), 1446.* https://doi.org/10.3390/rs15051446.

Khabarov, N., Krasovskii, A., Obersteiner, M., Swart, R., Dosio, A., San-Miguel-Ayanz, J., ... & Migliavacca, M. (2016). Forest fires and adaptation options in Europe. *Regional Environmental Change*, 16, 21-30. https://doi.org/10.1007/s10113-014-0621-0.

Kindermann, G. E., Schörghuber, S., Linkosalo, T., Sanchez, A., Rammer, W., Seidl, R., & Lexer, M. J. (2013). Potential stocks and increments of woody biomass in the European Union under different management and climate scenarios. *Carbon balance and management*, 8, 1-20. https://doi.org/10.1186/1750-0680-8-2.

Krasovskii, A., Khabarov, N., Migliavacca, M., Kraxner, F., & Obersteiner, M. (2016). Regional aspects of modelling burned areas in Europe. *International Journal of Wildland Fire*, 25(8), 811-818. https://doi.org/10.1071/WF15012.

Krasovskii, A., Khabarov, N., Pirker, J., Kraxner, F., Yowargana, P., Schepaschenko, D., & Obersteiner, M. (2018). Modeling burned areas in Indonesia: The FLAM approach. *Forests*, 9(7), 437. https://doi.org/10.3390/f9070437.

Kučerová, A., Rektoris, L., Štechová, T., & Bastl, M. (2008). Disturbances on a wooded raised bog—how windthrow, bark beetle and fire affect vegetation and soil water quality?. *Folia Geobotanica, 43(1), 49-67. https://doi.org/10.1007/s12224-008-9006-9.*

Pasztor, F., Matulla, C., Rammer, W., & Lexer, M. J. (2014). Drivers of the bark beetle disturbance regime in Alpine forests in Austria. *Forest Ecology and Management*, *318*, 349-358. https://doi.org/10.1016/j.foreco.2014.01.044.

Pasztor, F., Matulla, C., Zuvela-Aloise, M., Rammer, W., & Lexer, M. J. (2015). Developing predictive models of wind damage in Austrian forests. *Annals of Forest Science*, *72*, 289-301. https://doi.org/10.1007/s13595-014-0386-0.

Pucher, C., Neumann, M., & Hasenauer, H. (2022). An improved forest structure data set for Europe. *Remote Sensing,* 14(2), 395. https://doi.org/10.3390/rs14020395.

Radio Prague International. (2020, February 11). Prognosis: Bark beetle damage likely to double again next year. https://english.radio.cz/prognosis-bark-beetle-damage-likely-double-again-next-year-8108358.

Reimann, C. (2019, November). Bark beetles and storm fellings in central Europe: Effects on the market today and tomorrow. Deutsche Säge- und Holzindustrie Bundesverband e. V.

Robinne, F., Burns, J., Kant, P., de Groot, B., Flannigan, M. D., Kleine, M., & Wotton, D. M. (2018). International Union of Forest Research Organizations, 2018. Global fire challenges in a warming world. Occasional paper, (32). https://www.iufro.org/publications/occasional-paper-32-global-fire-challenges-in-a-warming-world.

Romagnoli, F., Cadei, A., Costa, M., Marangon, D., Pellegrini, G., Nardi, D., ... & Cavalli, R. (2023). Windstorm impacts on European forest-related systems: An interdisciplinary perspective. *Forest Ecology and Management,* 541, 121048. https://doi.org/10.1016/j.foreco.2023.121048.

Rossi, J. L., Komac, B., Migliorini, M., Schwarze, R., Sigmund, Z., Awad, C., ... & Thiebes, B. (2020). *Evolving Risk of Wildfires in Europe–Thematic paper by the European Science & Technology Advisory Group (E-STAG)* (Doctoral dissertation, UN Office for Disaster Risk Reduction (UNDRR)).

Sanginés de Cárcer, P., Mederski, P. S., Magagnotti, N., Spinelli, R., Engler, B., Seidl, R., ... & Schweier, J. (2021). The management response to wind disturbances in European forests. *Current Forestry Reports,* 7, 167-180. https://doi.org/10.1007/s40725-021-00144-9.

Seidl, R., Baier, P., Rammer, W., Schopf, A., & Lexer, M. J. (2007). Modelling tree mortality by bark beetle infestation in Norway spruce forests. *Ecological modelling*, *206*(3-4), 383-399. https://doi.org/10.1016/j.ecolmodel.2007.04.002.

Seidl, R., & Rammer, W. (2017). Climate change amplifies the interactions between wind and bark beetle disturbances in forest landscapes. *Landscape Ecology,* 32, 1485-1498. https://doi.org/10.1007/s10980-016-0396-4.

Tedim, F., Leone, V., & Xanthopoulos, G. (2016). A wildfire risk management concept based on a social-ecological approach in the European Union: Fire Smart Territory. *International Journal of Disaster Risk Reduction,* 18, 138-153. https://doi.org/10.1016/j.ijdrr.2016.06.005.

United Nations International Strategy for Disaster Reduction Secretariat (UNISDR), (2015). Sendai Framework for Disaster Risk Reduction 2015 - 2030.

U.S. Geological Survey (USGS), (1996). USGS EROS Archive - Digital Elevation - Global 30 Arc-Second Elevation (GTOPO30). https://doi.org//10.5066/F7DF6PQS.

Van Vuuren, D. P., Edmonds, J., Kainuma, M., Riahi, K., Thomson, A., Hibbard, K., ... & Rose, S. K. (2011). The representative concentration pathways: an overview. *Climatic change,* 109, 5-31. https://doi.org/10.1007/s10584-011-0148-z.

Wagner, C. V., & Pickett, T. L. (1985). *Equations and FORTRAN program for the Canadian Forest Fire Weather Index System,* Forestry technical report. Minister of Supply and Services Canada, Ottawa.

Warszawski, L., Frieler, K., Huber, V., Piontek, F., Serdeczny, O., Zhang, X., ... & Ge, Q. (2017). Center for international earth science information network—ciesin—columbia university. (2016). gridded population of the world, version 4 (gpwv4): Population density. palisades. ny: Nasa socioeconomic data and applications center (sedac). doi: 10. 7927/h4np22dq. Atlas of Environmental Risks Facing China Under Climate Change, 228.

Yang, X., Post, W. M., Thornton, P. E., & Jain, A. (2013). The distribution of soil phosphorus for global biogeochemical modeling. *Biogeosciences,* 10(4), 2525-2537. https://doi.org/10.5194/bg-10-2525-2013.